SHRP-A/UFR-92-612

A Differential Scanning Calorimetry Study of Asphalt Binders

Ian R. Harrison
G. Wang
T.C. Hsu
The Pennsylvania State University
Department of Materials Science and Engineering
325 Steidle Building
University Park, PA 16802

Strategic Highway Research Program
National Research Council
Washington, DC 1992

SHRP-A/UFR-92-612
Contract AIIR-05

Program Manager: *Ed Harrigan*
Project Manager: *Jack Youtcheff*
Production Editor: *Marsha Barrett*
Program Area Secretary: *Juliet Narsiah*

July 1992
Reprint December 1993

key words:
asphaltene
crystallization
calorimetric parameters
differential scanning calorimetry (DSC)
elution-adsorption chromatography fractions
enthalpy value
glass transition temperature
ion exchange chromatography (IEC)
linear paraffinic side chain
naphthene aromatics
polar aromatics
saturates
size exclusion chromatography (SEC)
thermal properties

Strategic Highway Research program
National Academy of Sciences
2101 Constitution Avenue N.W.
Washington, DC 20418

(202) 334-3774

50/NAP/1293

Acknowledgments

The research described herein was supported by the Strategic Highway Research Program (SHRP). SHRP is a unit of the National Research Council that was authorized by section 128 of the Surface Transportation and Uniform Relocation Assistance Act of 1987.

Contents

List of Figures

List of Tables

Abstract

This report examines the use of Differential Scanning Calorimetry (DSC) for studying the thermal properties and behaviors of asphalt. DSC was chosen over biaxial extension rheology testing, small angle laser scattering (SALS), and optical microscopy. These methods did not produce enough detail to reflect any variation in structure due to changes in thermal treatment. Whereas DSC provides parameters for comparing the: glass transition temperatures, endothermic behavior of asphalt fractions and whole asphalts; aging, slow cooling and heat rate effects of eight SHRP core asphalts and several other asphalts.

DSC testing of fractions based on their different chemical nature indicates that napthene aromatics contribute heavily to the endothermic effect of the parent asphalt. Polar aromatics show a small endothermic effect at similar temperature ranges. Asphaltene, due to its chemical nature, shows no endothermic effect. The thermal behavior of saturates is not clearly understood.

Analysis of the Size Exclusion Chromatography (SEC) fraction's DSC results show that the higher the molecular weight of the No. 1 fraction, the smaller the endothermic peak will be. This fraction is believed to be influenced by the high percentage of polycyclic aromatics in the asphalts. Analysis based on DSC results, composition data and molecular weight data for SEC and Ion Exchange chromatography (IEC) neutral fractions suggests that the average linear side chain length may be a key parameter affecting endothermic behavior.

Executive Summary

Originally, biaxial extension rheology testing, small angle laser scattering (SALS), optical microscopy and differential scanning calorimetry (DSC) methods were chosen to characterize the thermal properties of asphalt.

None of the methods except DSC provided enough detail in analyzing asphalt morphology. DSC did provide important parameters in studying the thermal behavior of asphalts. Therefore, the research focused on comparing the: glass transition temperatures; endothermic behavior of asphalt fractions and whole asphalts; aging, slow cooling and heat rate effects of eight SHRP core asphalts and several other asphalts.

Two different fractions varying in molecular size and molecular chemical nature were also tested to help understand the role of size and structure in affecting thermal behavior of whole asphalts.

All samples were preheated to 275±5°F for about five hours. A series of samples were subjected to hot and cold temperature cycles varying from -35°C to about 60°C to simulate different types of temperature changes.

Two DSC thermogram scans were taken during the process. Once after samples were alternately cooled from -60°C or -100°C then reheated to 100°C. The second scan was taken after the samples were again rapidly cooled from 100°C to -60°C or -100°C and then reheated to 100°C. The asphalt samples were fractionated using solvent deasphaltening, and elution-adsorption chromatography to obtain fractions of saturates, naphthene aromatics, polar aromatics and asphaltene. In addition, size exclusion chromatography fractions were studied; yet lacking molecular weight data further analysis was discontinued.

All the asphalts show a broad glass transition temperature ranging from -60°C to 0°C. Comparisons of the DSC scan information indicate that previous assumptions about the contribution of mixtures with various n-alkanes to the endothermic effect is not reflected in the DSC testing. Further analysis concludes that the length of linear paraffinic side chains affect the crystallization process. A correlation between molecular weight in relation to chain length is also indicated. Linear chains are longer the higher the molecular weight. Stable crystallization occurs in the presence of mononephthenic and/or aromatic linear side chains of some length. A high crystallinity may affect asphalts' mechanical properties by increasing: the hardness; the rubbery consistency and

the resistance to flow at high temperatures. These properties are highly desirable for many industrial applications.

The second scan did not show the well-defined peaks found in the first scan. The second scan indicates effects of crystallization within the asphalt by the lowered glass transition temperatures.

DSC tests on month-old samples to gauge the effects of age show additional molecule reorganization aided the increase of crystallization as seen by the reduced glass transition temperatures.

The DSC thermogram data was converted into ASCII and analyzed using newly developed computer programs for this study.

1. INTRODUCTION

The original purpose of this work was to characterize asphalts using a combination of techniques consisting of a biaxial extension rheology test, small angle laser scattering (SALS), optical microscopy and differential scanning calorimetry (DSC). From an early stage study, we found that SALS and optical microscopy are not sensitive enough to reveal a detailed phase morphology of asphalt and any variation of structure as a result of changing the sample thermal treatment. DSC did, however, prove to be useful in studying the thermal behavior of asphalts. It gives important parameters such as glass transition temperature, range of melting temperature of crystallites, and enthalpy of melting. Therefore, the major research was focused on studying thermal properties of some asphalts supplied by SHRP using DSC.

Thermal behavior of asphalts and their fractions have been investigated by a number of researchers [1-8]. Schmidt et al. [1], Connor and Spiro [2] were among the earlier researchers to study asphalt's glass transition temperatures with differential thermal analyzer (DTA). Other researchers [3-8] have used differential scanning calorimetry (DSC) in asphalts studies. Noel and Corbett [3] found that the glass transition and melting transition of asphalts were attributable to saturates and naphthene aromatic fractions. The molecular weight effect on the glass transition temperatures of asphalts has been studied by Huynh et al. [5]. More recently, Kumari [8] investigated the crystallization of asphalts using DSC and found that the exothermic heat content of asphalts were mainly dependent on the prior cooling time rather than on the thermal history of the samples.

In this project, the basic thermal properties of eight SHRP core asphalts and several other asphalts have been determined. Two different types of fractions obtained, based on molecular size and molecular chemical nature, were tested to help understand the role which fractions of different sizes and chemical structures assume in governing the thermal behavior of whole asphalts. The influences of different thermal histories on asphalt thermal behaviors were also studied. DSC results, compared with composition data, seem to suggest that the saturates fraction content is not the dominant factor that affects the endothermic behavior as previously reported [3,7]. Furthermore,

analysis indicates that the average linear side chain length is one of the key parameters affecting the endothermic peak size.

In this report, the thermal properties of asphalts and several fractions tested will be presented and analyzed.

2. EXPERIMENTAL AND PROCEDURE

2.1 Sample Preparation

All asphalts were preheated following the MRL(Material Reference Library) protocol to 275± 5°F for about five hours to ensure uniformity of composition. DSC samples were prepared under argon filled gas bags to protect the asphalts from being oxidized. Due to the sticky nature of asphalts, Teflon film was used to move the asphalt into an aluminum pan. Usually 15 to 25 mg asphalt samples were used. Prepared DSC samples were stored in an argon gas bag for at least three days before being tested.

In order to simulate temperature variations during a day and night cycle, we prepared a series of asphalt samples using a heating-cooling device to change the sample environment temperature from -35°C to about 60°C at a frequency of 5 minutes per cycle for different periods of time ranging from several days to one month. Also, samples were stored in a refrigerator at -30±4°C for different periods of time to explore the effect of cooling on asphalt thermal properties. Several samples for slow cooling study were made by heating first to 100°C and subsequently cooling to room temperature at a cooling rate of 1.5°C/hr.

2.2 DSC Testing

DSC tests were conducted with a Perkin-Elmer 7500 DSC instrument calibrated at 20°C/min against indium. Helium was used as the purging gas when the tests started from -100°C; Argon when starting from -60°C.

All samples were loaded into the sample cell at 30°C and subsequently rapidly cooled down to -60°C or -100°C at a cooling rate of 200°C/min. The sample remained at the low temperature for about 15 minutes to ensure a

stabilized initial reading. It was then heated to 100°C at a heating rate of 20°C/min. The DSC thermogram recorded during this heating scan is designated as the first scan. On completing the first scan, the sample was quickly cooled from 100°C to its starting temperature (-60°C or -100°C) at a cooling rate of 200°C/min and again held for about 15 minutes before being reheated to 100°C at a heating rate of 20°C/min. The DSC thermogram recorded during this second heating scan is designated as the second scan.

DSC thermogram data were transferred into ASCII format using Perkin-Elmer's software in order to perform more detailed analysis on an IBM PS/2 computer. Calorimetric parameters were calculated using a newly developed computer program for this study.

3. RESULTS AND DISCUSSION

In this section the basic features of asphalts' DSC scans and some definitions used in analysis are introduced first. DSC results of two types of asphalt fractions are then presented and analyzed in order to better understand the thermal behavior of the whole asphalts. After that, the melting behavior of eight SHRP core asphalts are discussed in conjunction with their composition data and the molecular weight data of two different fractions. The influence of different thermal treatments on asphalts' thermal behavior are discussed thereafter.

3.1 Basic Characteristics of Asphalts' DSC Scans and Definitions of Reported Parameters.

Basic characteristics of asphalts' DSC scans can be typically represented by an AAM-1's DSC curve shown in Figure 1. All the asphalts show a broad glass transition temperature ranging from -60°C to 0°C. Following the glass transition are two endothermic peaks overlapping each other somewhat. The two endothermic peaks usually have their peak temperatures at about 15°C and 45°C, respectively. DSC scans of different asphalts may appear to have different shapes due to variations in intensity of the melting peaks or shifts of the peak positions to higher or lower temperatures.

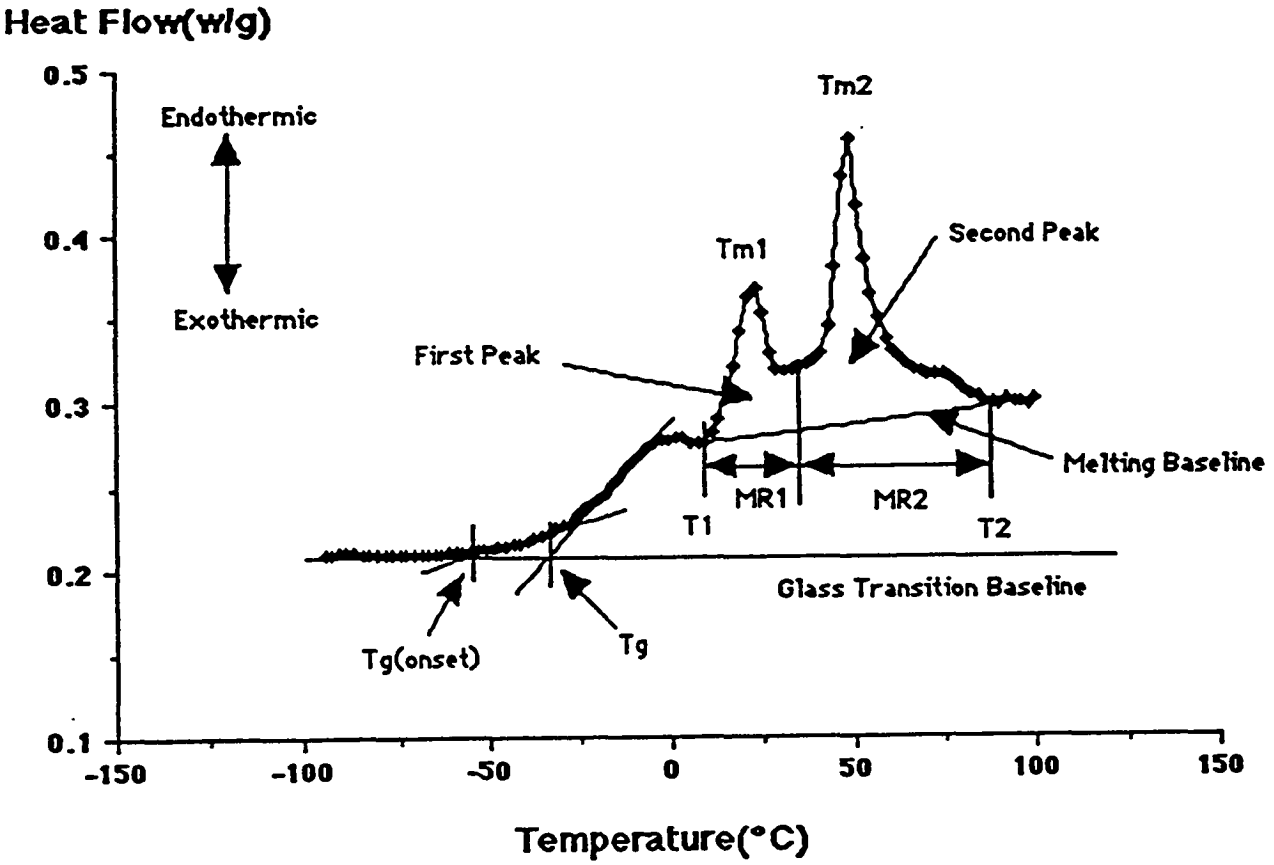

Figure 1. Typical Asphalt's DSC Scan and Some Definitions Used in Analysis.

Figure 1 also shows some definitions of basic thermal properties and terms that are used in our analysis. The glass transition baseline in an "as performed" DSC scan is usually not horizontal and instead has a positive slope. The DSC scan shown in Figure 1 is a horizontally aligned thermogram. The alignment procedure is designed to add or subtract a constant slope to the whole thermogram until the slope of the pre-glass transition baseline is zero (see Appendix). Since many asphalts show quite different slopes within the glass transition region, careful labeling of the glass transition temperatures is necessary. Tg_{onset} and main Tg are, therefore, calculated in our analysis. The sloping lines used to calculate Tg_{onset} and Tg are again obtained by linear regression over selected data points.

Although we sometimes see a minor exothermic effect immediately after the glass transition, we did not attempt to quantitatively analyze it due to the difficulty in determining its position and intensity. Construction of the melting baseline, as shown in Figure 1, is performedly connecting the starting and end

point of the melting peaks. The dividing line between the two melting peaks is set at the approximate mid-point of the flat portion between Tm1 and Tm2. A small shoulder following the second peak seen in many asphalts' DSC scans was not recorded as an independent peak, instead, this component was considered as part of the second peak. Tm1 and Tm2 represent the peak temperatures of the first and second melting peaks. MR1 and MR2 represent the melting range of the two melting peaks. T1 and T2 are the starting and ending temperatures for the whole melting event.

Considering the complexity of asphalt compositions, DSC data obtained in this research has shown a fairly good reproducibility. The data fluctuation for Tg_{onset} and Tg are within ±2°C; Tm1 and Tm2 are not very reproducible for samples with weak and broad endothermic peaks; but for samples with relatively large and well defined peaks these values vary within ± 2°C. ΔH is very sensitive to the baseline selection and since asphalt do not exhibit well defined, clear cut melting peaks, this value may involve more subjective judgement. Nevertheless, for asphalts with relative large melting peaks such as AAM-1, AAB-1 and AAF-1, the fluctuation of this value is within ± 10%; for asphalts with small melting peaks it can be as much as ±15%.

3.2 Thermal Behavior of Asphalt Fractions

3.2.1 Solvent Deasphaltening, Elution-adsorption Chromatography Fractions

Since asphalts are mixtures of various hydrocarbons of different chemical structures and molecular weights, it is necessary to know how different asphalt compositions play a role in determining the overall thermal behavior of whole asphalts. Fractions of AAG-1 and AAK-1 were tested which had been separated using solvent deasphaltening, elution-adsorption chromatography. Due to the nature of the separation technique, these fractions (saturates, naphthene aromatics, polar aromatics and asphaltene), can be considered to have reasonably distinct chemical structures.

Four DSC scans of AAK-1's fractions are shown in Figure 2 and the basic thermal properties are listed in Table 1. The saturates fraction shows an unusual response. Considering that crude oils have Tg values ranging from -80 to -120°C [6], the thermal event at -75°C could be the glass transition. The big

exothermal thermal peak next to the glass transition is most likely the result of crystallization of small paraffin molecules and the broad endothermic peak represents the melting of the crystallites formed during cooling and heating.

Both naphthene aromatics and polar aromatics fractions have Tg_{onset} near -60°C. The onset of Tg is clearly due to low molecular weight materials existing in both fractions. Their main glass transition temperatures, however, are quite different. Naphthene aromatics has a relatively low, sharp glass transition while the polar aromatics shows a broader and higher glass transition. This can be related to differences in their chemical structure, molecular weight and molecular weight distribution. Naphthene aromatics are yellow to red liquids consisting of paraffin, naphthene aromatics and other sulfur-containing compounds with a typical number average molecular weight of about 725 [9]. Polar aromatics, on the other hand, have higher molecular weight which is typically about 1150 and contain some aromatics in multi-ring structures as well as paraffin and naphthene aromatics. The higher main Tg transition of polar aromatics is probably caused by the higher molecular weight and more rigid nature of multi-ring molecular structures. Hon Kiet Huynh et al. [5] have found an increase in Tg as the molecular weight of asphalt fractions increases from about 800 to 3000.

Endothermic peaks Have been found to be more prominent in naphthene aromatics than in polar aromatics. Two major melting peaks can be easily identified in the naphthene aromatics' DSC thermogram. Between these two melting peaks a small peak can also be seen.

Asphaltene fraction, containing mixed paraffin-naphthene-aromatics in polycyclic structures, shows a simple DSC scan with a very broad Tg transition and a tiny endothermic peak at a much higher temperature than that of the melting peaks found in naphthene aromatics. If this fraction consists of pure polycyclic aromatic material, then, there should be no endothermic event occurring within this testing temperature range. The observed small endothermic peak is most likely due to the crystallizable "impurities".

AAG-1's three fractions show similar behavior as AAK-1's except that AAG-1's asphaltene fraction shows no sign of endothermic effect (see Figure 3).

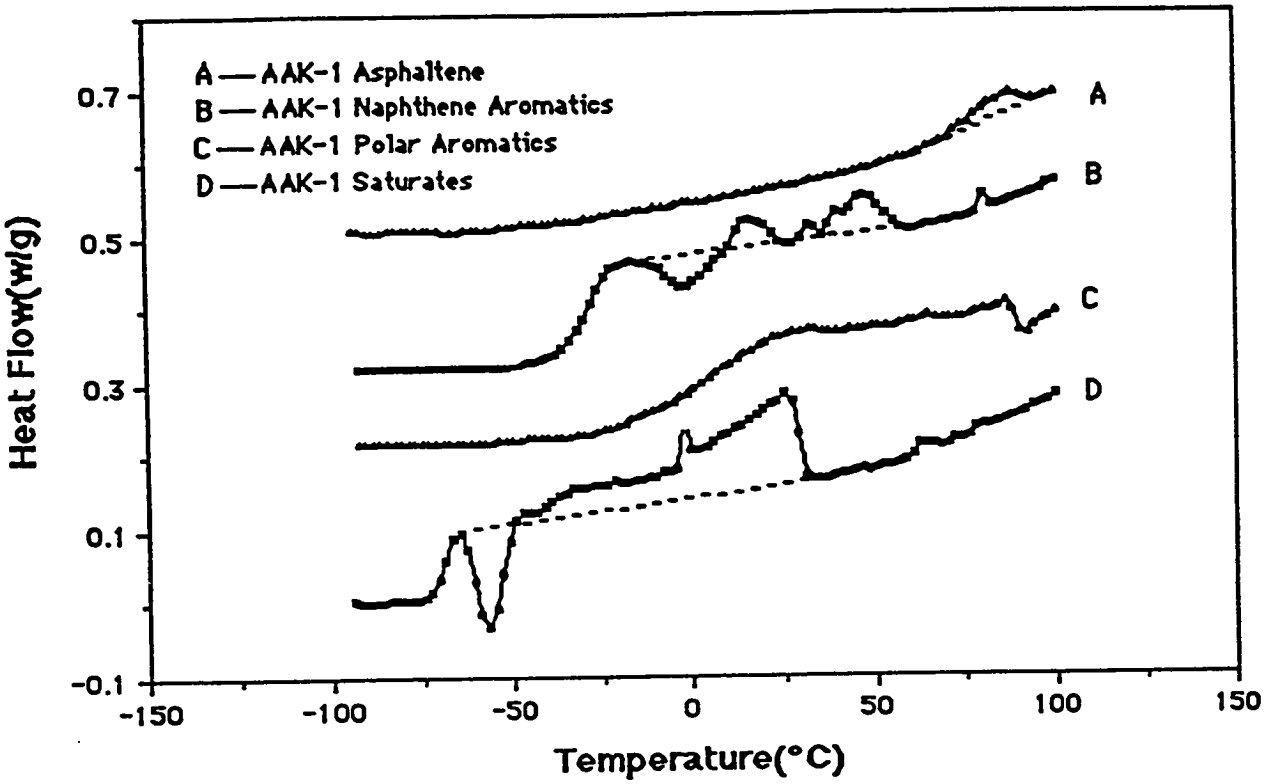

Figure 2. DSC curves of AAK-1's fractions

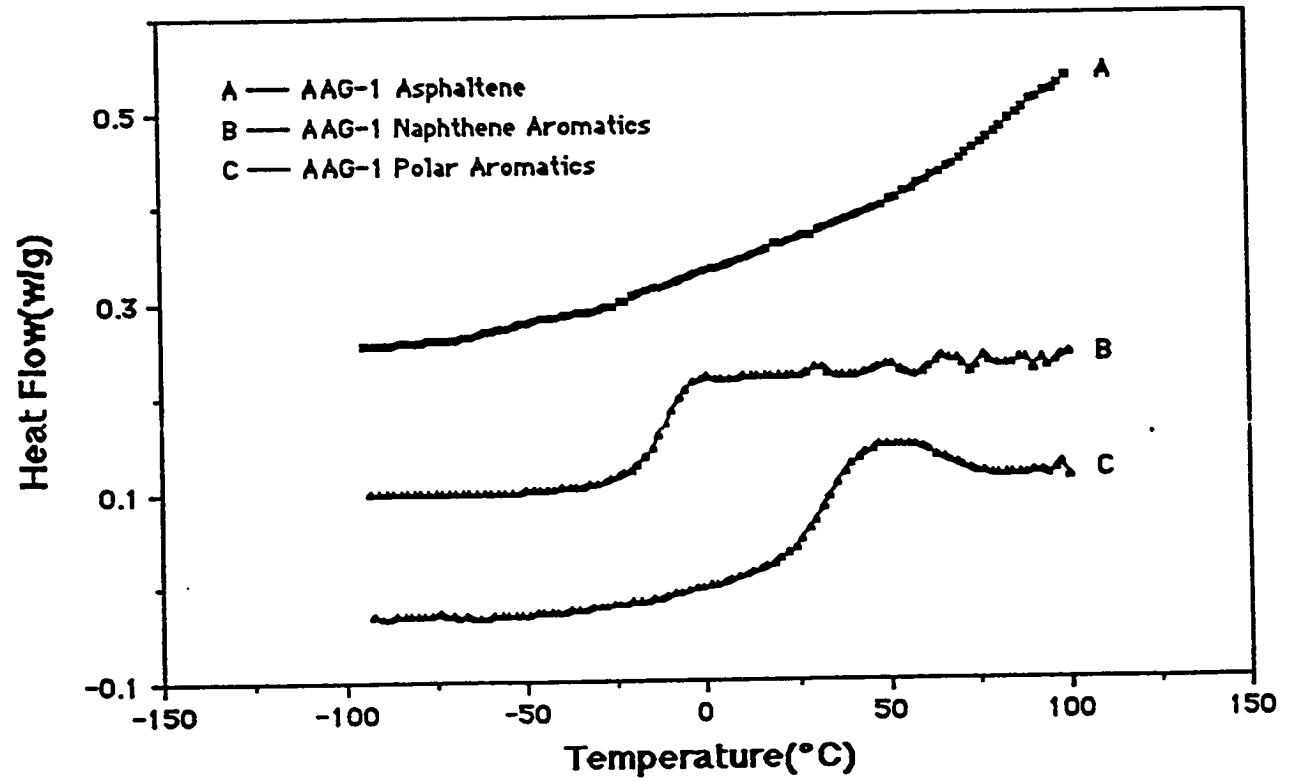

Figure 3. DSC curves of AAG-1's fractions.

Table 1. Thermal properties of AAK-1 fractions.

Fraction(%)	Tg(°C) (onset)	Tg(°C) (main)	ΔH (J/g)	ΔH1 (J/g)	ΔH2 (J/g)	Tm1 (°C)	Tm2 (°C)
Asphaltene	-	-	0.65	-	-	-	-
Polar Arom.	-60.0	-18.5	1.42	-	-	-	-
Nap. Arom.	-59.2	-37.9	6.65	3.14	3.51	14.7	47.2
Saturates	- 75.0	-72.4	22.40	-	-	-	-25.2

3.2.2 Size Exclusion Chromatography (SEC) Fractions

The thermal properties of another type of fraction of AAC-1, AAK-1 and AAM-1 have also been studied. Three pairs of DSC scans of SEC fractions of asphalt AAC-1, AAK-1 and AAM-1 are shown in Figure 4 and their thermal properties are listed in Table 2. Molecular weight data of these particular fractions has not been supplied to us at this time. Without this information, further discussion is fruitless. Fortunately, data for presumably similar asphalt fractions have been published by Branthaver et al. [10].

It is observed that all No.1 fractions show much weaker endothermic effects than the corresponding No.2 fractions. From Table 3, we see that all No.1 fractions of the three asphalts have significantly higher number average molecular weights than the corresponding No.2 fractions. Comparing these data with DSC scans shown in Figure 4, we see a simple correlation between the molecular weight and the melting effect, i.e., the fractions with lower molecular weight show more prominent endothermic effect than those with higher molecular weight. For example, AAC-1's No.2 fraction has two well defined major endothermic peaks plus a shoulder peak and its No.1 fraction shows only a negligible endothermic sign at around 80°C. Similarly, AAK-1's No.2 fraction shows distinct endothermic peaks while its No.1 fraction only has a small one at higher temperature position. AAM-1's No.2 fraction also shows higher melting peaks than its No.1 fraction although the difference between the two AAM-1's fractions is much smaller. Of course, the molecular weight difference between the two AAM-1's fractions is also much smaller than the differences in AAC-1 and AAK-1 fractions.

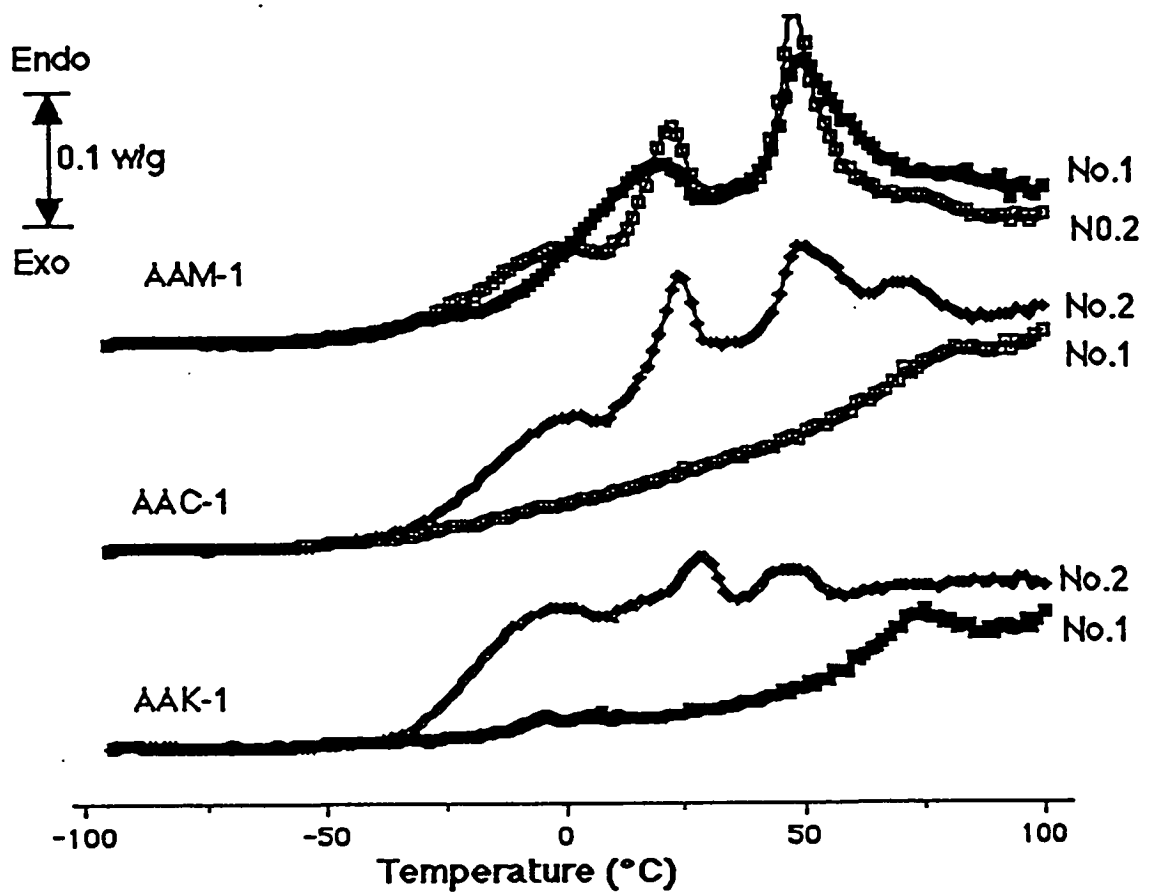

Figure 4. DSC curves of SEC fractions of AAC-1, AAK-1 and AAM-1

Table 2. Thermal Properties of SEC Fractions of AAC-1, AAK-1 and AAM-1

Thermal	AAC-1		AAK-1		AAM-1	
Parameters	No.1	No.2	No.1	No.2	No.1	No.2
Tg_{onset} (°C)	-61.2	-60.5	-60.3	-60.7	-59.4	-61.0
Tg (°C)	-40.5	-33.7	-	-34.3	-44.8	-35.3
ΔH_{total}	1.19	9.87	1.18	2.11	14.11	10.79
ΔH_1	-	3.22	0.43	1.28	5.77	3.36
ΔH_2	1.19	6.65	0.75	0.83	8.34	7.43
Tm_1	-	24.8	-3.7	28.8	19.2	22.9
Tm_2	78.4	49.1	75.2	46.1	50.1	48.5
MR1	-	26.7	41.3	28.3	50.7	26.1
MR2	44.5	49.8	22.4	21.6	58.4	50.4
T1	49.3	9.1	-12.8	9.3	-18.7	9.3
T2	93.8	85.3	89.6	58.1	90.1	85.7

Table 3. MW Data for Preparative SEC Fractions [10]

Asphalt	Fraction Number					
	1	2	3	4	5	6
AAA-1	11,000	2,200	1,200	730	540	390
AAB-1	9,200	1,800	1,000	710	550	430
AAC-1	7,380	1,610	1000	780	610	490
AAD-1	7,000	2,200	1,200	700	470	360
AAF-1	8,690	1,970	1,100	770	610	480
AAG-1	7,900	1,700	990	710	550	420
AAK-1	10,000	1,700	1,000	650	410	340
AAM-1	4,600	1,700	1,100	810	600	480

* MW values are number-average MW's obtained by VPO in toluene at 60°C.

As we know, SEC fractions are obtained based on different molecular sizes and may or may not represent different molecular structures. The above observation, however, clearly indicates that different molecular weight fractions from the same asphalt are indeed different in molecular structures. The higher molecular weight fractions contain more species with polycyclic aromatic structures [3, 9]. Therefore, they show weak endothermic effects similar to the asphaltene and polar aromatics fractions discussed in 3.2.1 section. Additional evidence to support that it is molecular structure, rather than molecular size, that determines asphalt melting behavior, comes from a comparison between the No.2 fractions of the three asphalts. The three No.2 fractions have approximately the same molecular weights, yet AAM-1's No.2 fraction shows a much larger endothermic effect than the two others.

Another difference between No.1 fractions and No.2 fractions is reflected by DSC scans, namely, No.2 fractions display a more distinct and narrower glass transition than No.1 fractions. Clearly, the distinct glass transition for No.2 fractions is due to a relatively large amount of smaller molecules present in these fractions which have lower Tgs. In contract, No.1 fractions mainly consist of larger molecules and only a small amount of low molecular weight components are present. The larger molecules in No.1 fractions might also be strongly associated together and therefore have a broader glass transitions. The Tg_{onset} of No.1 fractions reflect the low Tg of those smaller molecules.

The small endothermic peaks found in No.1 fractions of both AAK-1 and AAC-1 could be a glass transition phenomenon or a sign of real melting. However, since a small melting peak (shoulder peak) has been found in No.2 fractions in approximately the same temperature range, it is believed that this represents a real melting peak.

3.3 Thermal Behavior of Whole Asphalts

3.3.1 Glass Transition

DSC curves of eight SRHP core asphalts are shown in Figure 5 and their thermal property data are listed in Table 4. With the exception of AAG-1 which has a significantly higher Tg_{onset} and main Tg value, the rest of the core asphalts have Tg_{onset} at about -60°C and the main Tg around -43 °C. The Tg_{onset} temperature is more closely related to the glass transition temperature of the saturate fraction that has the lowest Tg. The main Tg reflects characteristics of the glass transition temperatures of the majority of components.

Since Tg is a material's characteristic temperature at which all molecular translational motion is "frozen", the material become rigid and brittle at or below this temperature. The Tg is believed to be closely related to the low temperature performance of asphalts. Based on Tg values, we might expect that in the low temperature region (roughly between -40 and 0°C) AAG-1 exhibits a more brittle nature than other asphalts. It would be difficult to speculate on the low temperature performance of other asphalts because they do not have significant differences in Tg.

3.3.2 Endothermic Behavior

When comparing total endothermic enthalpy values ($\Delta H_1+\Delta H_2$), we did not see the same simple relationship as that of Tg. Each asphalt has its own characteristic enthalpy value. AAM-1 has the greatest while AAA-1 the smallest. In general, AAM-1, AAB-1 and AAF-1 have much higher enthalpies than the rest (see Figure 6).

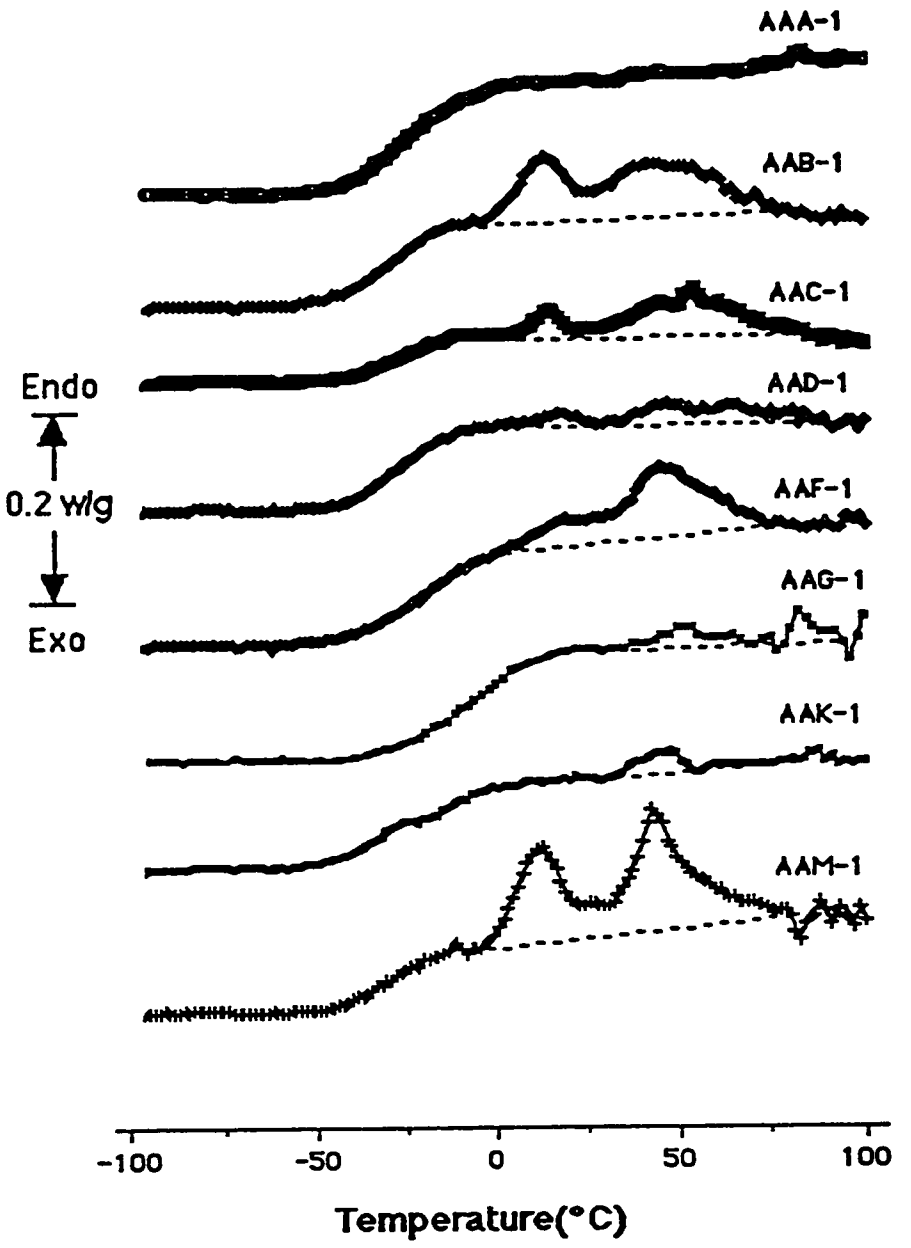

Figure 5. DSC curves of eight SHRP core asphalts.

Table 4. The Thermal Properties of Eight SHRP Core Asphalts

	AAA-1	AAB-1	AAC-1	AAD-1	AAF-1	AAG-1	AAK-1	AAM-1
Tg_{onset}(°C)	-59.2	-59.9	-54.8	-59.4	-60.3	-46.4	-59.6	60.1
Tg(°C)	-42.6	-44.7	-42.1	-42.8	-40.2	-27.7	-45.2	-44.4
ΔH_{total}(J/g)	0.27	9.94	4.00	3.48	7.93	2.42	1.83	12.86
ΔH_1(J/g)	-	3.30	0.65	0.76	1.73	1.29	-	5.14
ΔH_2(J/g)	0.27	6.64	3.35	2.72	6.20	1.13	1.83	7.69
Tm_1(°C)	-	13.9	15.5	19.5	18.7	51.7	-	12.0
Tm_2(°C)	83.5	41.9	53.9	46.1	44.8	82.9	47.2	42.7
MR1(°C)	-	30.7	24.3	33.2	29.3	34.7	-	33.9
MR2(°C)	19.9	62.9	58.4	61.3	56.5	26.9	-	52.8
T1(°C)	70.1	-4.5	1.3	-3.5	-1.9	33.6	-	-6.4
T2(°C)	90.0	89.1	84.0	90.9	84.8	95.2	-	80.26

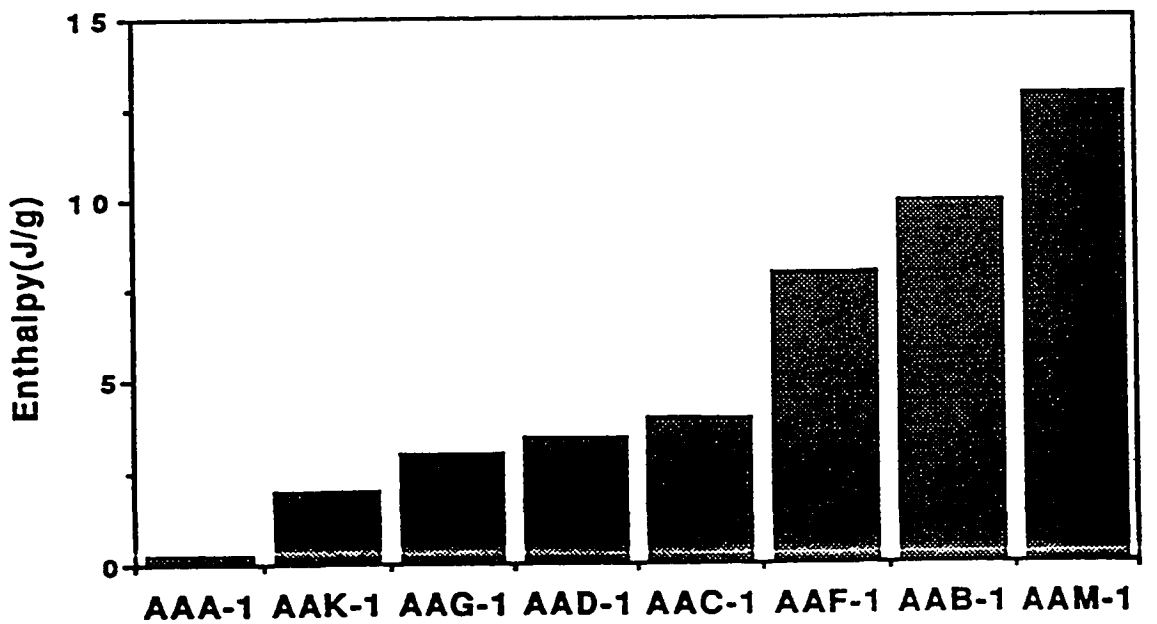

Figure 6. Endothermic Enthalpies of Eight Core Asphalts.

Molecular origins of the endothermic events It is not an easy task to accurately determine the molecular origins of the thermal events of asphalts observed in DSC curves without first knowing the composition and molecular structure of asphalts. Since asphalts are such complicated systems

composition analysis only gives approximate information. Composition data of eight asphalts listed in Table 5 gives percentages of four types of fractions in each asphalt: asphaltene, polar aromatics, naphthene aromatics and saturates. The molecular sizes and structures of eight core asphalts revealed by the molecular weights of SEC fractions.

Table 5. The Composition Data of Eight SHRP Core Asphalts

Fraction(%)	AAA-1	AAB-1	AAC-1	AAD-1	AAF-1	AAG-1	AAK-1	AAM-1
Asphaltene (n-heptane)	18.3	18.2	11.0	23.0	14.1	5.8	21.1	3.9
Polar Aromatics	37.3	38.3	37.4	43.1	38.3	51.2	41.8	50.3
Naphthene Aromatics	31.9	33.4	37.1	25.1	37.7	32.5	30.0	41.9
Saturates	10.6	6.6	12.9	8.6	9.6	8.5	5.1	1.9

* This information is supplied by the Asphalt Research Program Center For Transportation Research.

It is widely believed that saturates, which are basically a mixture of various n-alkanes, contribute most to the endothermic effect [3,7]. However, from our DSC testing we did not see a good agreement. From Table 5 we see that AAM-1, among the eight core asphalts, has only 1.9% saturates content, yet shows the most prominent endothermic effect. While AAG-1, having a much higher saturate content and with other compositions similar to that of AAM-1, showed only a trace endothermic effect. AAA-1, has a very similar composition to that of AAB-1 except for a somewhat larger saturates content, yet AAA-1 showed almost no endothermic effect, whereas AAB-1 did show a much larger one. Based on this observation, it seems that saturates content is not the dominant factor that determines the magnitude of the endothermic effect. This apparent contradiction to anticipated behavior might be due to the relatively small amount of saturates present in these asphalts. Although saturates are normally easily crystallized at lower temperatures and show an endothermic peak when subjected to heating, the low percentage present in asphalts is probably not enough to dominate the thermal behavior of the whole asphalts.

If saturate content is not the dominant factor governing the endothermic behavior then, what is the key component that contributes most to the whole asphalt endothermic effect? Is it the polar aromatics that made a great contribution to the AAM-1 asphalts' endothermic peak? If so, then why does AAG-1, with a higher polar aromatics content, only display a trace of endothermic effect? In fact, other studies [3,7] and our own DSC testing (see section 3.2.1) have show that polar aromatics are not responsible for the endothermic peaks. We know naphthene aromatics are crystallizable; but, are the naphthene aromatics the major fraction that determines the thermal behavior of the whole asphalt? From Table 5, we see that those asphalts which have shown large endothermic effects only contain slightly higher naphthene aromatics. Again, AAG-1, with almost the same percent naphthene aromatics as AAB-1, has an enthalpy less than a quarter of AAB-1's. Therefore, correlation of endothermic effects with composition data based on four fractions can not be easily established. Other molecular parameters need to be considered in order to understand the thermal behavior of asphalts.

Paraffinic side chain length One such critical parameter is believed to be the length of linear paraffinic side chains in paraffin-naphthene-aromatic molecules. Irregular bulky ring structures can not easily fit into crystal structures rather, they disrupt the crystallization process. Not all linear paraffinic side chains are capable of crystallizing; only those with enough chain length would be able to form crystallites. This point has been clearly illustrated in Figure 7.

Comparing DSC results with the molecular weights of SEC fractions seems to support this point. AAM-1's No. 1 SEC fraction has a much smaller molecular weight compared to that of the other asphalt's No. 1 fraction. Since all the measurements were made using the same column, the smaller MW of AAM-1's No.1 fraction means that the average molecular structure of AAM-1 No. 1 fraction is more linear because linear molecules have higher hydrodynamic volumes than that of other types of molecules.

In addition, the molecular weights of neutral fractions, obtained by ion exchange chromatography (IEC) [11] and listed in Table 6, more specifically indicate that the chain length of naphthene aromatics of AAM-1, AAB-1 and AAF-1 are much longer than that of others. It has been demonstrated that the highest MW fractions of an asphalt contain most of the polar strong acid and

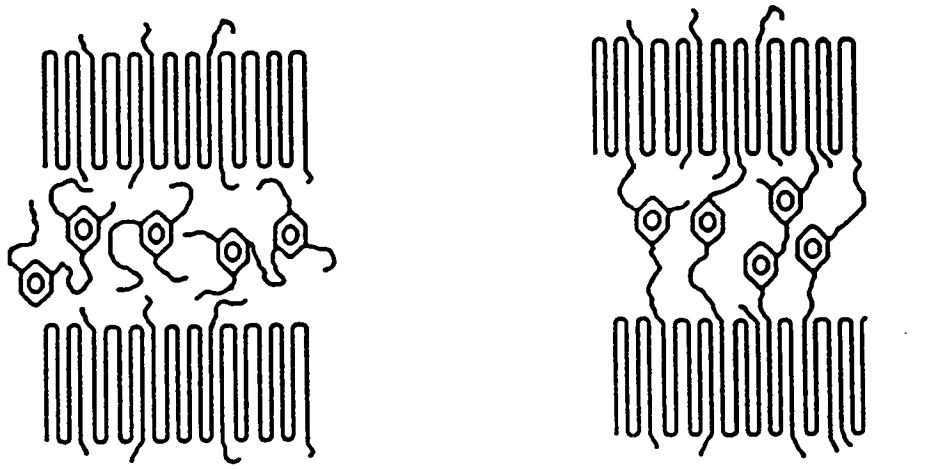

Crystals made of linear paraffin molecules (a)

Crystals made of long linear side chains (b)

Figure 7 Schematic illustration of possible crystallites formed by side chains of naphthene aromatics structures and linear paraffin molecules.

Table 6. Molecular Weights of IEC Neutral Fractions [11]

Asphalt Neutral Fraction	Molecular Weight (Daltons)
AAA-1	590
AAB-1	660
AAD-1	510
AAF-1	700
AAG-1	590
AAK-1	590
AAM-1	1,140

strong base components [11]. Therefore, the IEC neutral fraction basically represents mixtures of paraffins and paraffin-naphthene-aromatics. The higher the molecular weight of this fraction, the longer the linear chains will be.

The relatively small difference in the molecular weights between IEC neutral fraction of AAB-1 and AAA-1 and the large difference between their melting peaks might be explained with the number and position of the mono nephthenic and/or aromatic groups on linear side chains. If these bulky groups

are mostly located at the end of the chain, the portion of the undisrupted chain suitable for crystallization will be longer. Otherwise, this undisrupted linear chain might be too short to be able to crystallize.

The influence of crystallites on asphalts' performance The influence of crystallites and their melting behavior on the whole asphalts' mechanical properties is of practical importance. For example, a high crystallinity may increase the hardness and bring about a more rubber-like consistency and a better resistance to flow at high temperatures. These properties are highly desirable for many industrial applications such as coating cables, adhesives, covering terraces and so on [6].

The crystallite contents or crystallinities of asphalts, which are proportional to the enthalpy values, are very small compared to that of most crystalline polymers. It has been reported [7] that only a few percent to 11% crystallizable materials are present in asphalts. We would not expect a dramatic influence on asphalts' performance resulted from such small amount of crystallites which act simply as rigid fillers (see Figure 7 (a)). However, if crystallites in the asphalt matrix are not made up solely of linear paraffin molecules but also incorporate linear paraffinic side chains from molecules with naphthene-aromatic ring structures, then crystallite influence might be much greater than anticipated. In fact, it is clearly that in the case of AAM-1, linear paraffinic chains in naphthene aromatics are the major crystallizable materials. In this case, the crystallites act as physical crosslinks rather than just as rigid fillers (see Figure 7(b)).

For a semi-crystalline polymer, at temperatures below Tg, crystallites tend to make the material more brittle possibly due to strain, stress concentration brought about by crystallites; at temperatures between Tg and the melting temperature, crystallites act as rigid fillers and physical crosslinks which increase a material's modulus, tensile strength and elongation to break. For asphalts, since their crystallinities are very low we do not anticipate a significant brittle effect produced by crystallites at temperature below Tg. However, we may see some effect at temperatures above the glass transition but below the melting temperature. For example, as the temperature increases, the decrease of the elastic modulus of asphalts with more crystallites might be considerably slower due to the physical crosslink effect of crystallites; the elastic modulus may vary with temperature according to the melting pattern shown in DSC thermograms.

Figure 8 schematically shows the possible variation pattern of elasticity modulus in the melting temperature range. After glass transition, the elastic modulus for pure amorphous asphalts falls quickly to a very low level. For a crystalline asphalt, crystallites acting as physical crosslinks make the asphalt with higher elastic modulus. As temperature increases, crystallites with melting temperatures corresponding to the first melting peak in the DSC scan begin to melt and cause the elastic modules to drop because the number of physical crosslinks is decreased. At the end of the first melting peak the rate of melting decreases and the drop of elastic modulus become slower; the elastic modulus drops more rapidly again at temperatures corresponding to the second melting peak. Finally, when all crystallites melt the elastic modulus falls to the same level as that of pure amorphous asphalt.

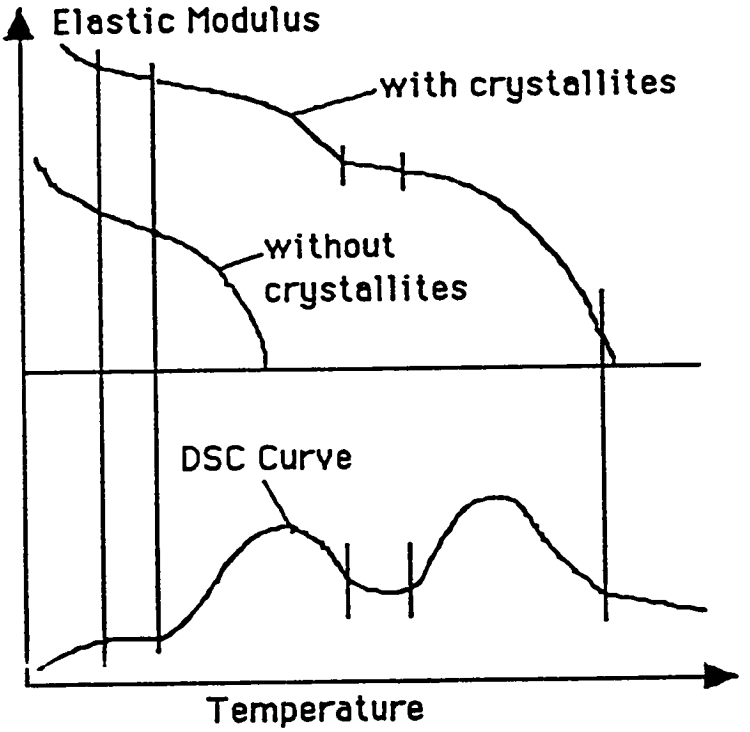

Figure 8 Schematic illustration of possible relationship between elastic modulus and temperature for crystalline asphalts.

It should be pointed out that making prediction about mechanic properties of asphalts purely based on the enthalpy value might not be appropriate. Many other factors, such as molecular weight, molecular structures etc., may also affect asphalts' properties. However, the enthalpy value of

asphalt does provide an important clue in understanding certain asphalts' properties and should not be neglected.

3.4 Comparison Between First Scan and Second Scan

Figure 9 shows several pairs of first run and second run DSC curves. It can be seen that the second run generally does not show as well defined peaks as those found in the first scan. Instead, a new broad 'peak', which is more like a glass transition curve, can be seen at the position where melting peaks are located in the first run. In most cases, the glass transition temperature of the second run is several degrees lower than that of the first run. The exothermic effect shown in the second run is usually much bigger than the one shown in the first scan.

The differences between the first and second runs might be due to fast cooling from their molten state to low temperature. When the first heating is finished the asphalt is in a molten state, i.e., all crystallites were melted and mixed with the non-crystallizable materials. A sudden, fast cooling will prevent those crystallizable materials from appreciable crystallization. As a result, when the asphalt sample is brought down to its starting low temperature it contains only small crystallites. Due to fast cooling, a "looser", more highly strained asphalt matrix structure will be formed. Because of these structural variations in the asphalt matrix, its Tg value is expected to be lower. The bigger exothermic effect in the second run is due to the crystallization of those crystallizable materials which fail to crystallize during the fast cooling process. Possibly the release of strain energy, which was stored in the asphalt matrix during the cooling process, may also make a contribution to this exothermic effect.

The broadness of the peak of the second run is probably related to cocrystallization of different crystallizable molecules. Cocrystallization results in imperfect crystallites which have lower melting temperatures. These imperfect crystallites will melt again as temperature increases, and the higher molecular weight fractions also may recrystallize and remelt again. This would result in a broader but decreased peak spanning over the whole melting temperature range of the first run. In fact, it is observed that most of the peak temperatures of the second scan are located at lower temperatures than those of the first melting peak of the first run.

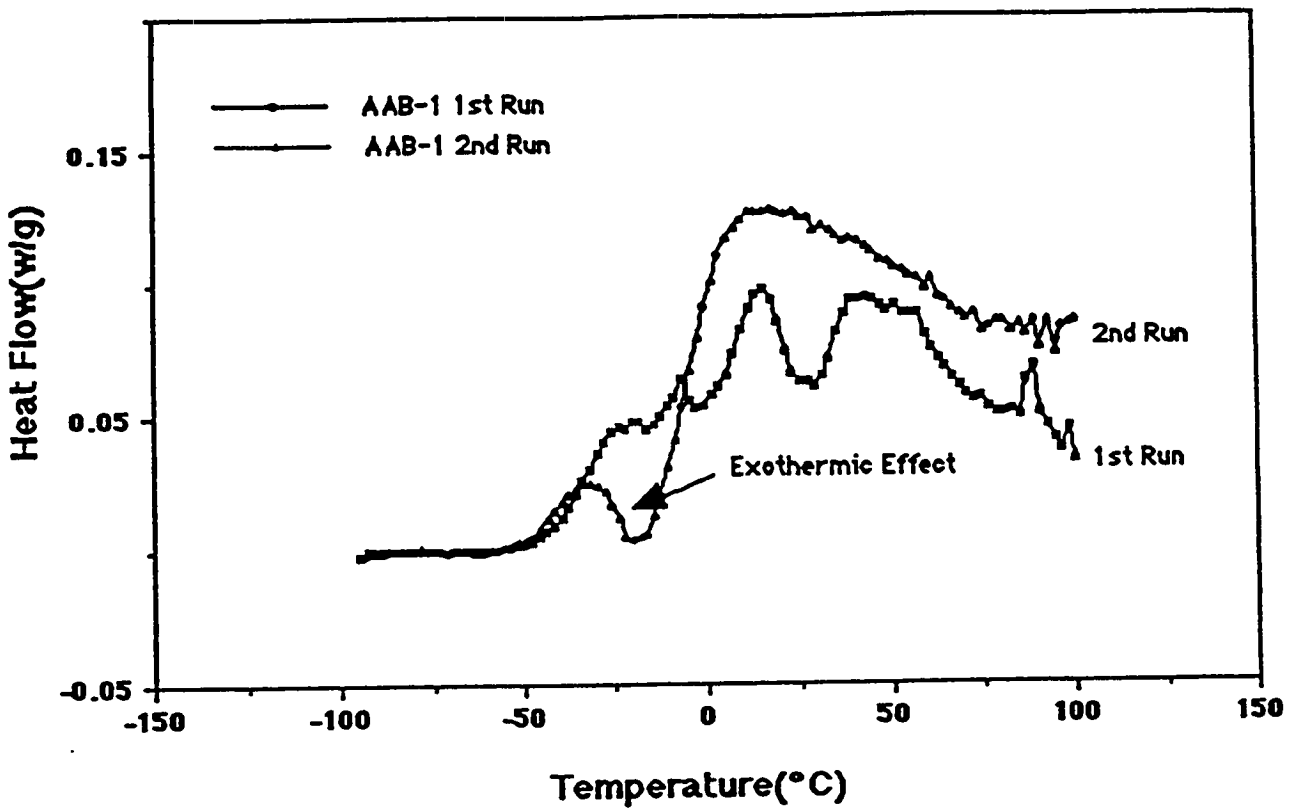

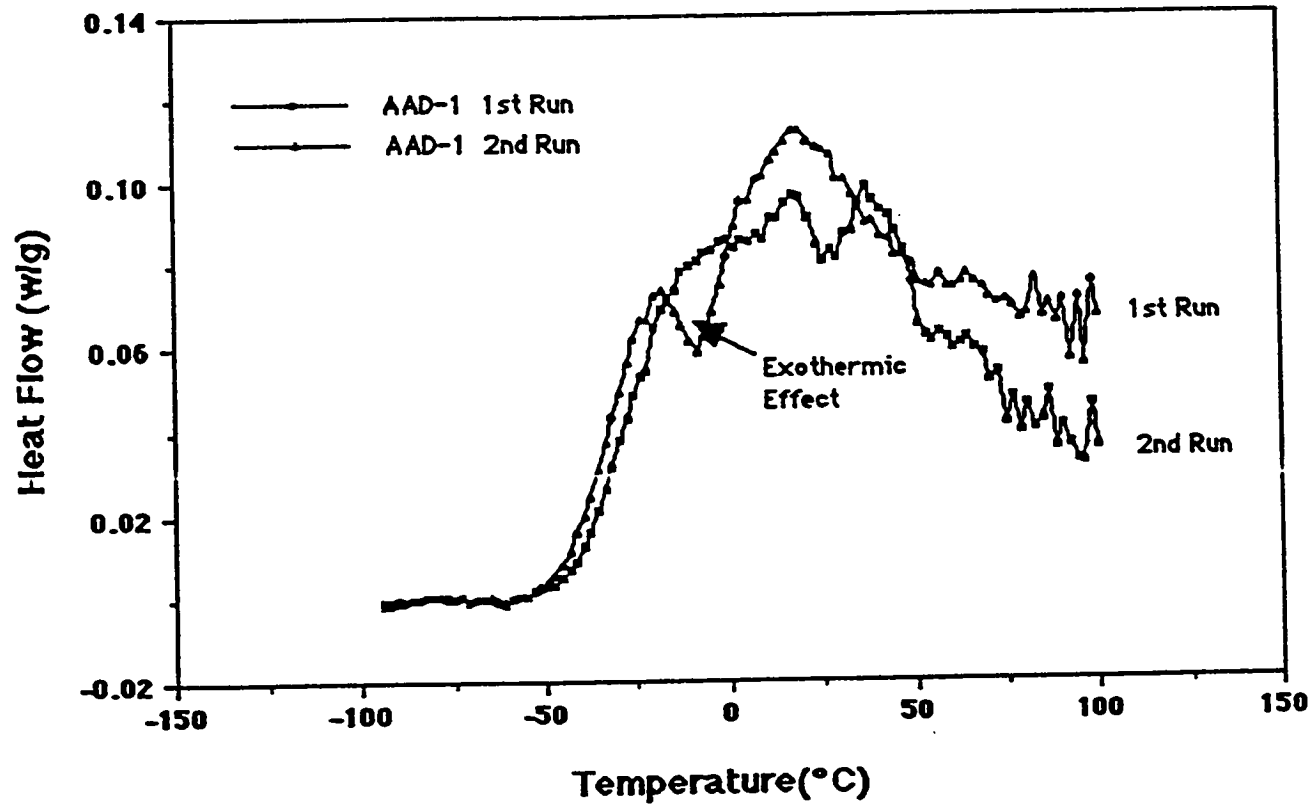

Figure 9. DSC curves of first and second runs (to be continued).

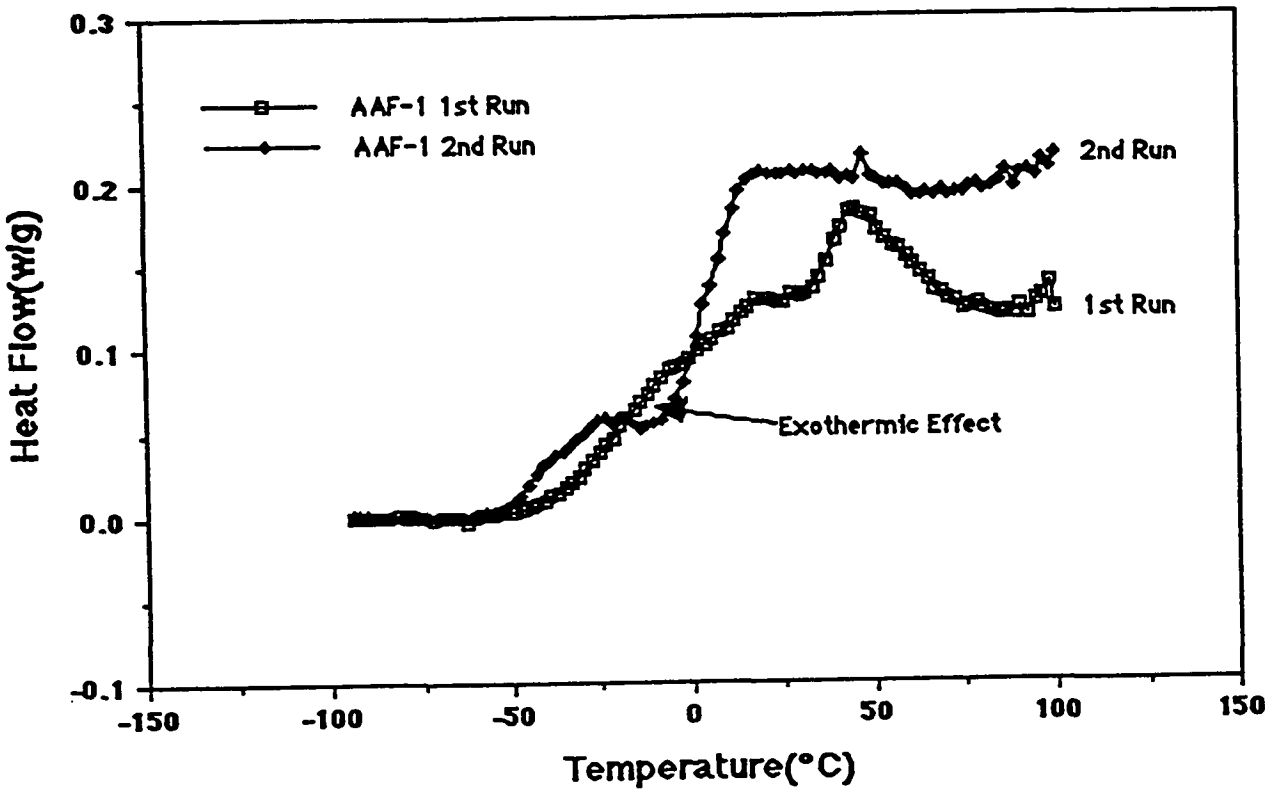

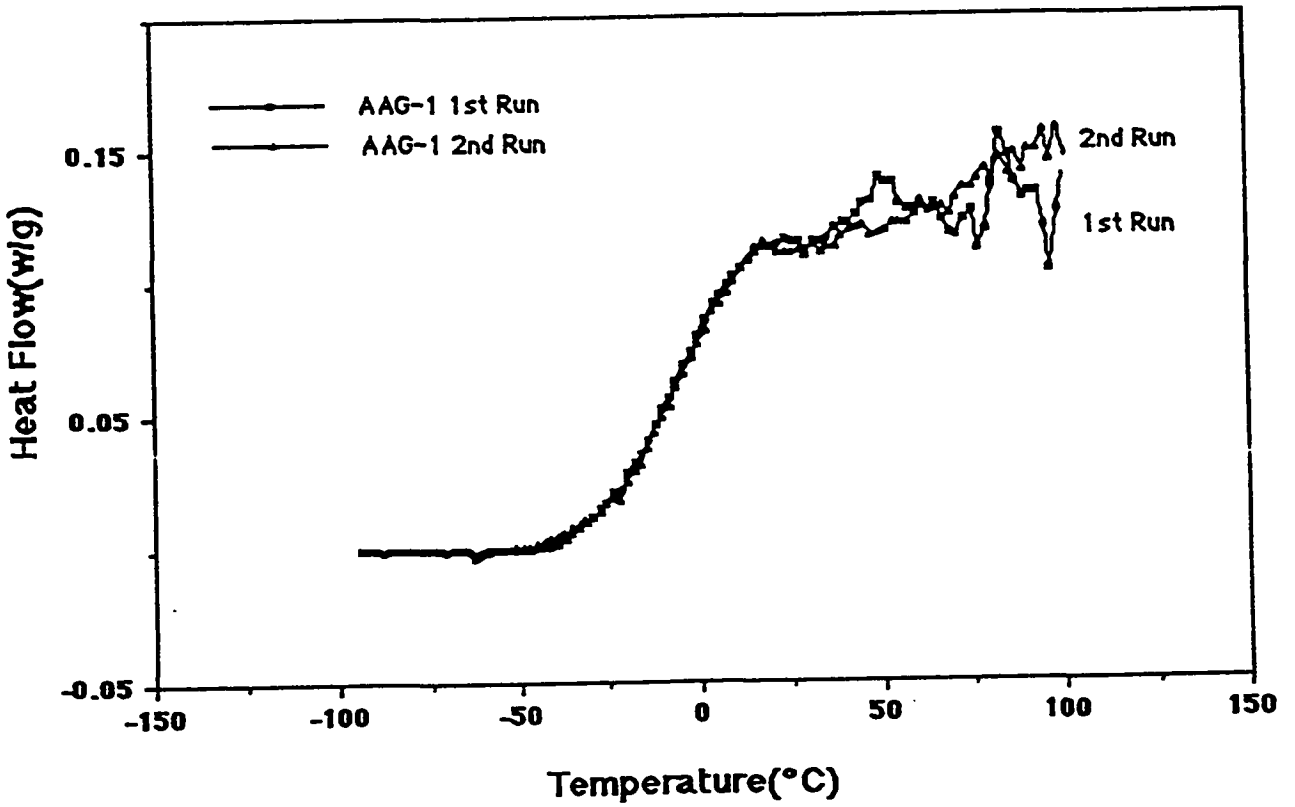

Figure 9. DSC curves of first and second runs (to be continued).

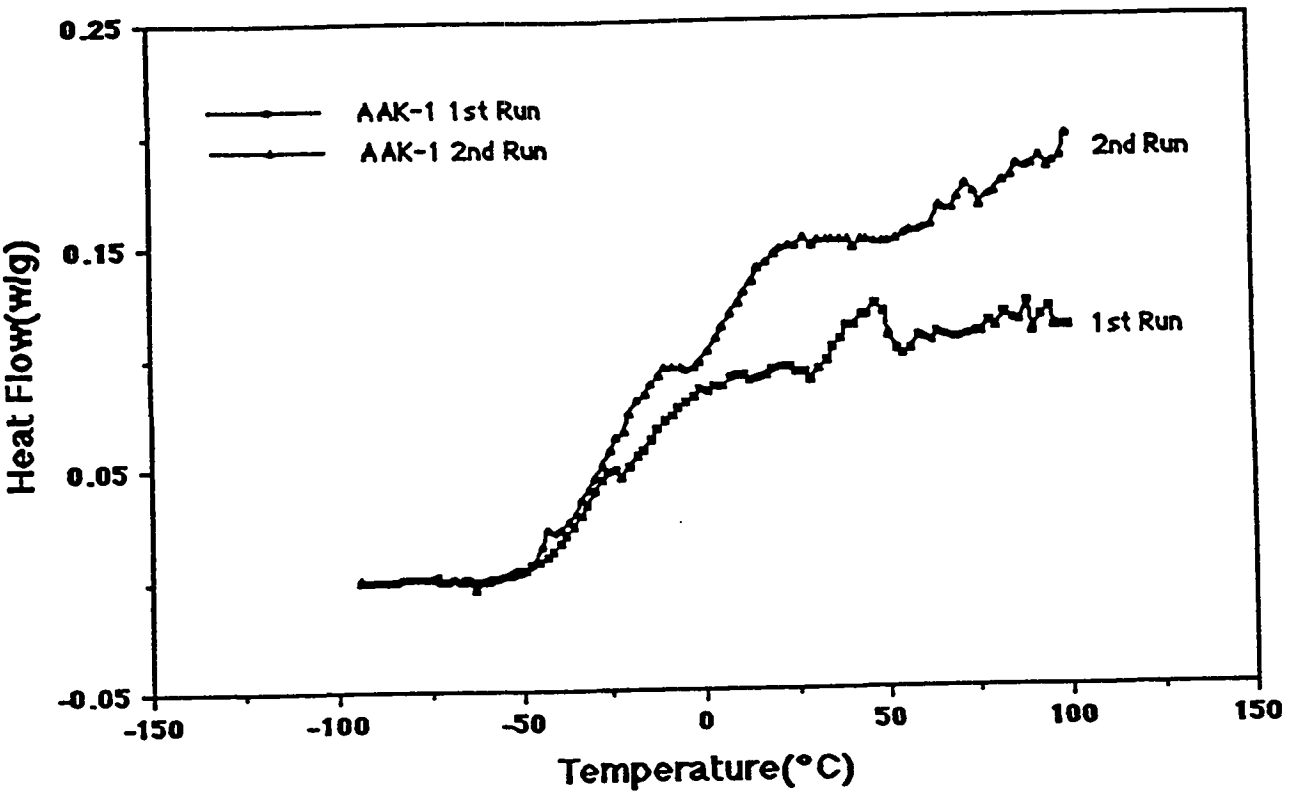

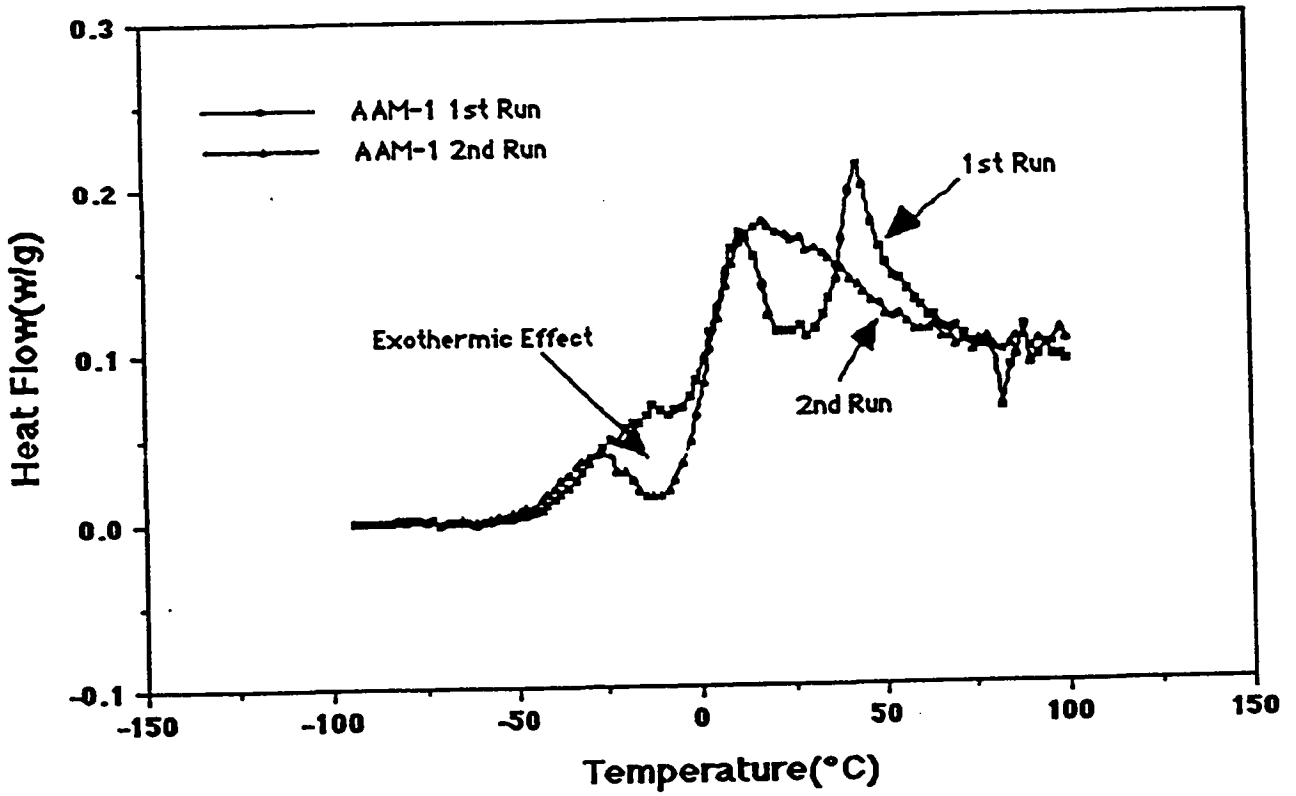

Figure 9. DSC curves of first and second runs.

3.5 Aging Effect Study

One of the important aspects about asphalts is the effect of aging on their thermal behavior. We did some DSC tests to check if there were any variations in DSC scans. Samples used in this experiment had already been tested and then stored at room temperature in air for one month. The DSC testing condition was the same as the original run except argon was not used for the re-run. Since samples were kept in the original DSC pan it is believed that they were free from contamination. If there is any variation in the re-run it must be due to an aging effect.

The DSC scans from the re-run tests show some interesting differences which vary with different asphalts. First, we observed that almost all the re-run tests show that Tg starts at approximately 5°C lower than the original run. This effect is clearly displayed in the derivative curves (see Figures 10, 11). We are not sure about the cause of this Tg lowering. One interpretation might be that oxidation reduces some of the molecular size and, therefore, increases the proportion of smaller molecules. This, in turn, would enlarge the glass transition range and lower the starting point of Tg.

Another interesting feature observed from the re-run DSC scans is that melting peaks become narrower, sharper and more cleanly separated (less overlap). Considering sample thermal history difference, we tend to believe that reorganization of molecules could be the major factor. For the original tests, samples were heated to melt and then stored at room temperature for only two days. Samples may not have had enough time to reach their most stable state. Many smaller molecules, which could be separated from the larger ones if they had enough time, were still retained within structures containing predominantly larger molecules when originally tested. These smaller or defective molecules would interrupt crystallization of other crystallizable materials, thereby, causing broad endothermic peaks. For the re-run tests, smaller molecules in the samples had enough time to phase separate, and at the same time the crystallizable fraction became relatively pure and, therefore, formed better crystals which, in turn, resulted in narrower and sharper peaks.

Figures 12 and 13 show a comparison of the original run and re-run DSC curves for AAM-1 and AAD-1. The AAM-1 had more observable narrowing and sharping effects than AAD-1. This is presumably due to the fact that AAM-1 has much more crystallizable materials than AAD-1.

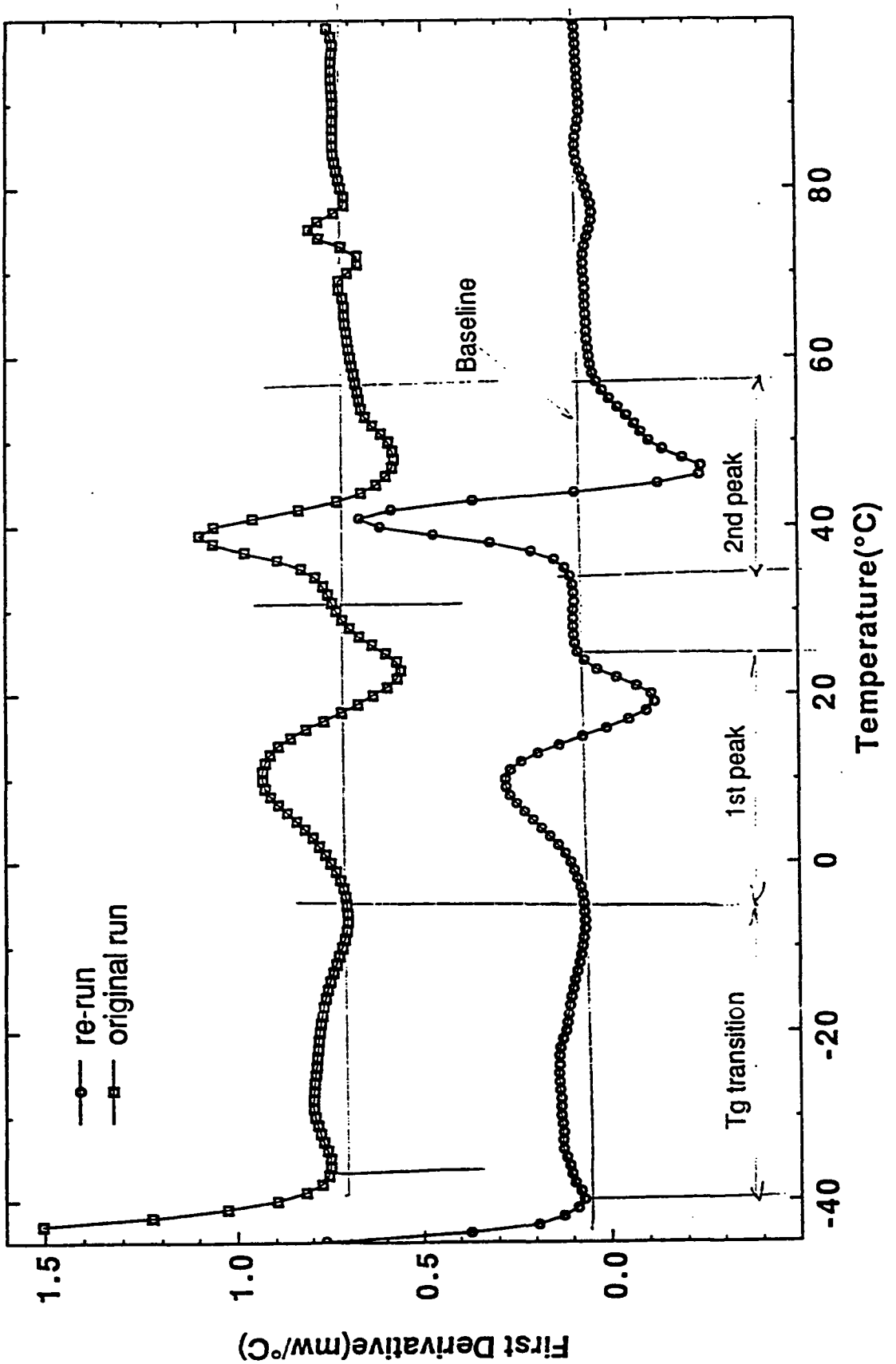

Figure10. AAM Derivative Curves

Figure11. AAD Derivative Curves

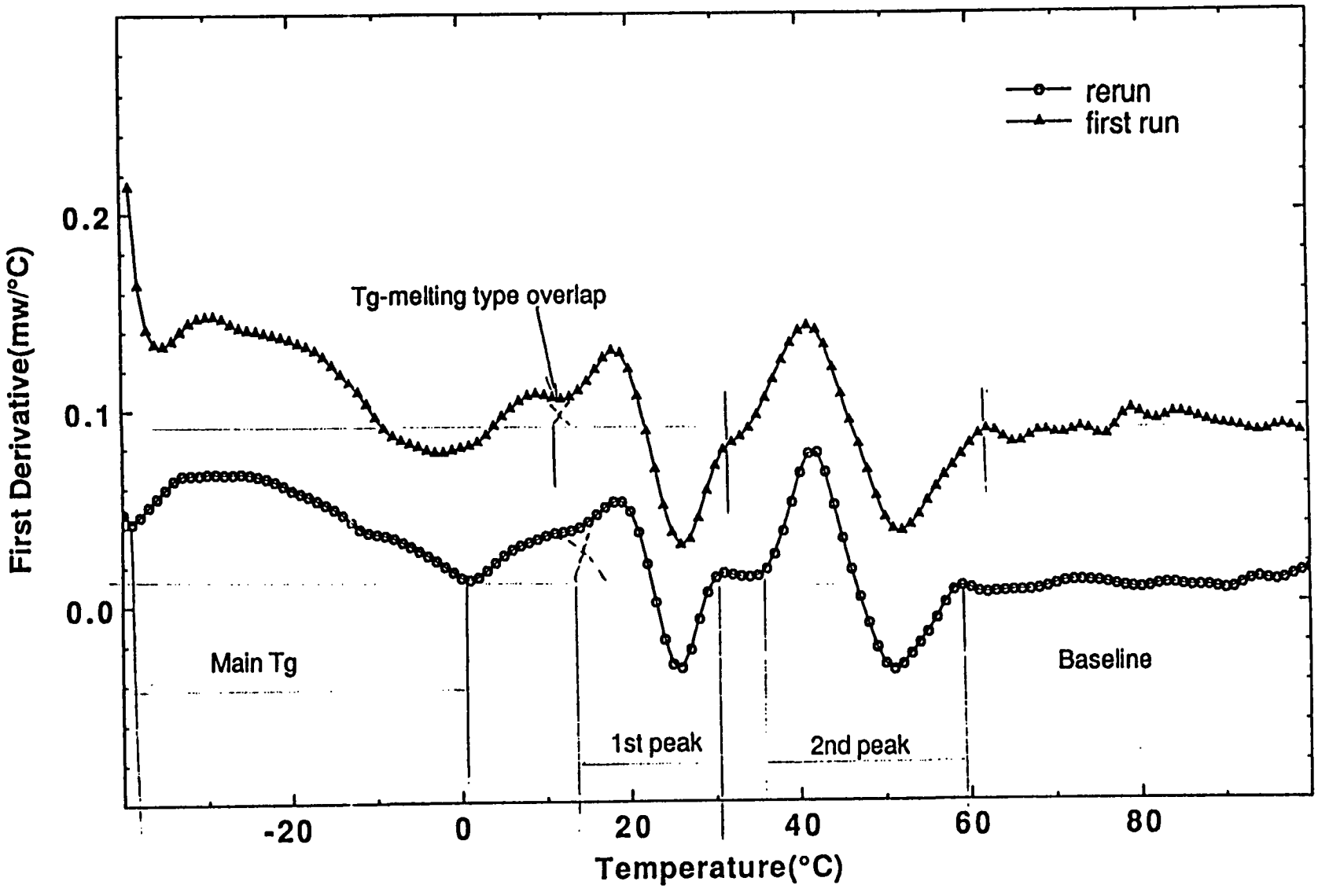

Figure 12. AAM DSC Curves

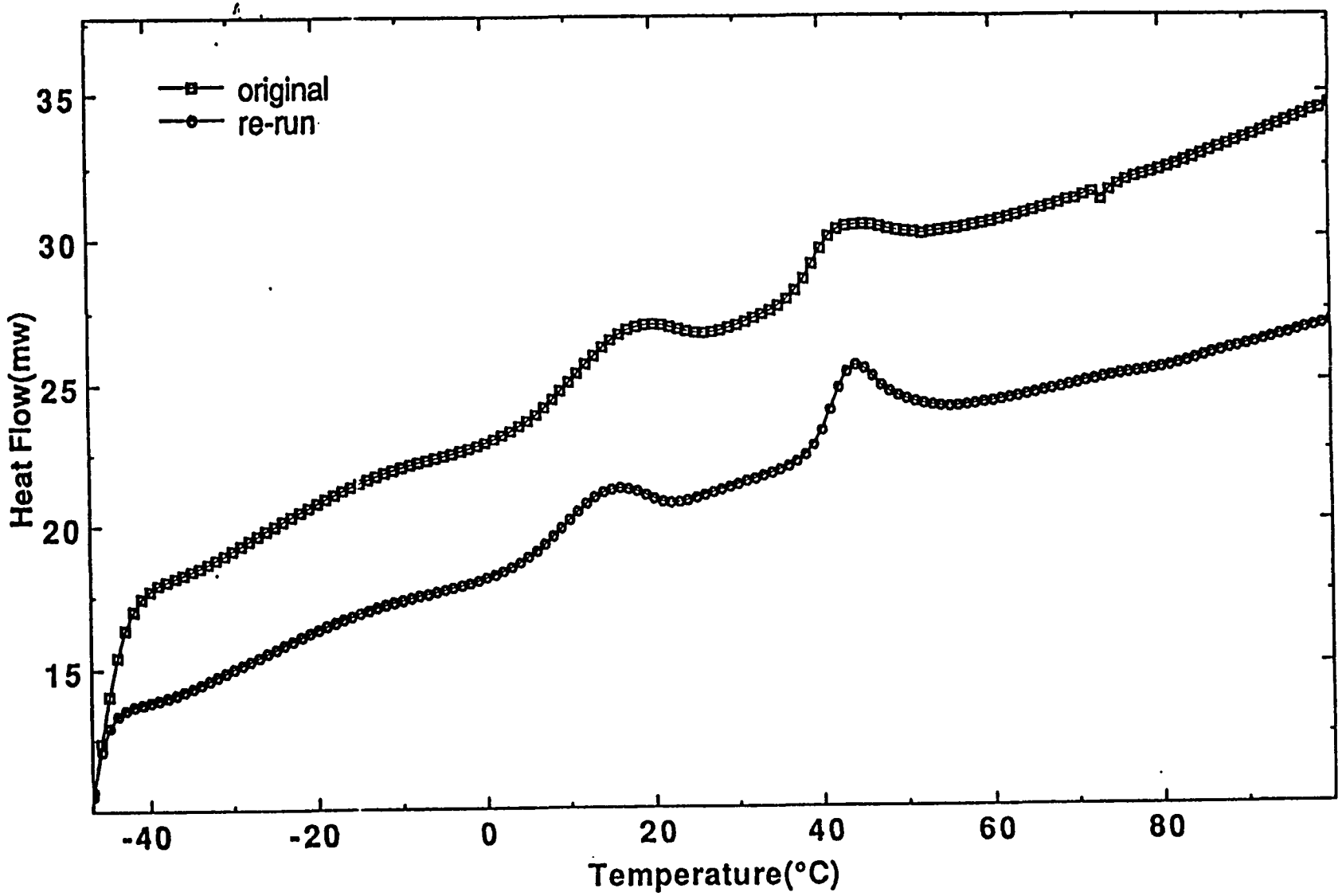

Figure 13. AAD DSC Curves

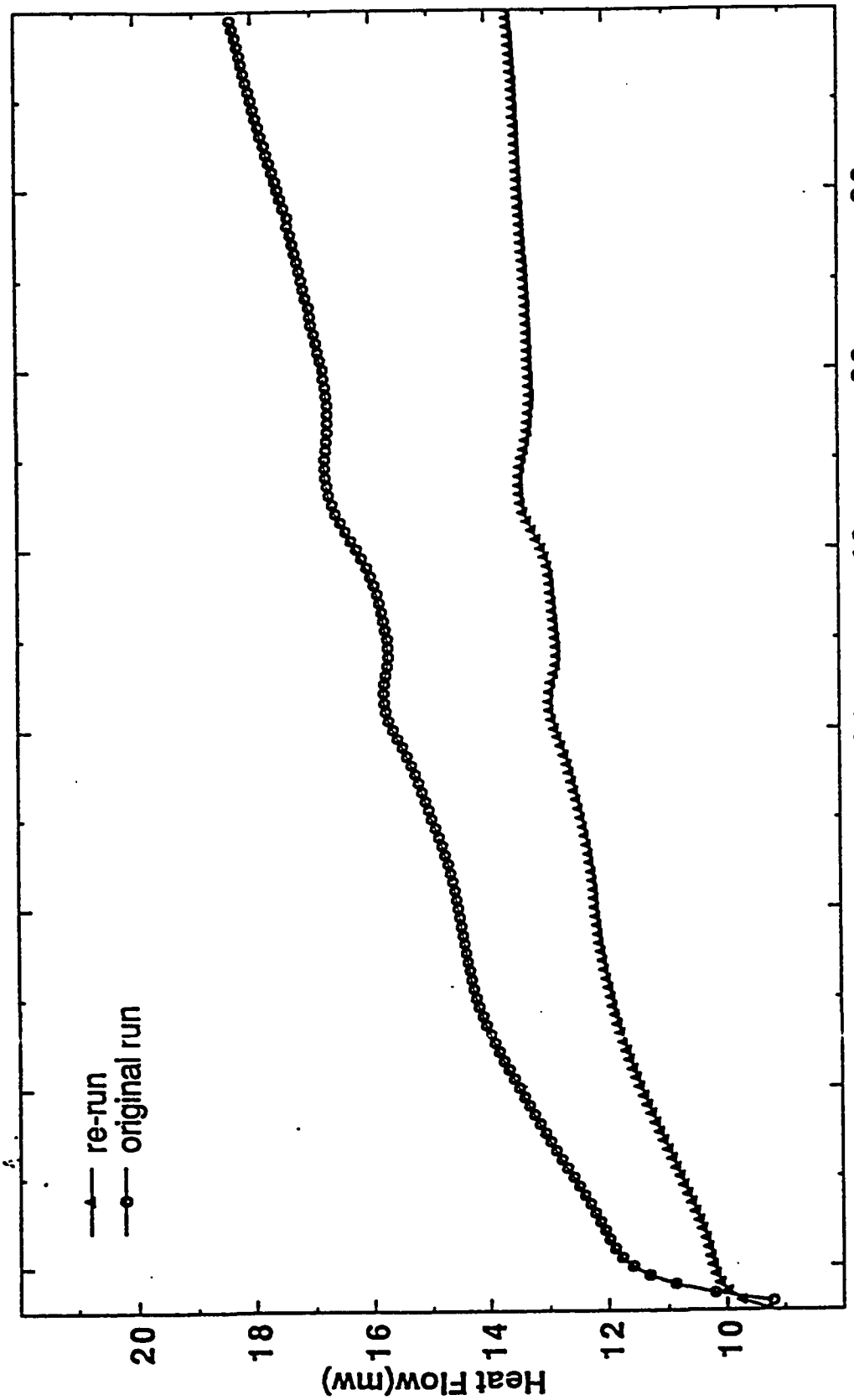

Figures 14 and 15 show comparison curves for AAK-1 and AAX. These curves demonstrate a very puzzling feature: the first endothermic peak has disappeared. The second endothermic peak, like those in AAM-1 and AAD-1, becomes sharper and can still be explained as the result of molecular reorganization. The tough question is why did the first peak largely disappear. After being thoroughly reorganized, molecules which were responsible for the first peak may have formed crystals which are so stable that they effectively joined materials which form the second peak.

3.6 Slow Cooling Effect

Several samples have been made by first melting the asphalts at 100°C and slowly cooling to room temperature at a rate of 1.5°C/hr. We expected that samples treated in this fashion would show different thermal behavior within the cooling temperature range than those cooled normally to room temperature. Slowly cooled sample did not show an increase in melting enthalpy, however, the peak position did change a little bit. The first peak shifted to a lower temperature and the second peak shifted to a higher temperature. The separation between the first peak and the second peak is greater and the high temperature shoulder has been separated much better from the second peak. Figure 16 shows DSC curves of slowly cooled AAM-1 and room temperature cooled AAM-1. Since cooling was from 100°C to about 30°C, the first peak was not expected to be affected. The first peak shifting is probably simply due to better separation which causes all large crystallizable molecules to form higher melting crystals and the smaller crystallizable molecules to form lower melting crystals.

3.7 Heating Rate Effect

Heating rate is one of the parameters that can affect DSC results significantly. Three heating rates have been tested. The major thermal properties of AAM-1 measured at different heating rates are listed in Table 7. It can be seen that the first endothermal peak area increases significantly as the heating rate decreases from 10°C/min to 5°C/min, but the total enthalpy did not

Figure 14. AAK1 DSC curve

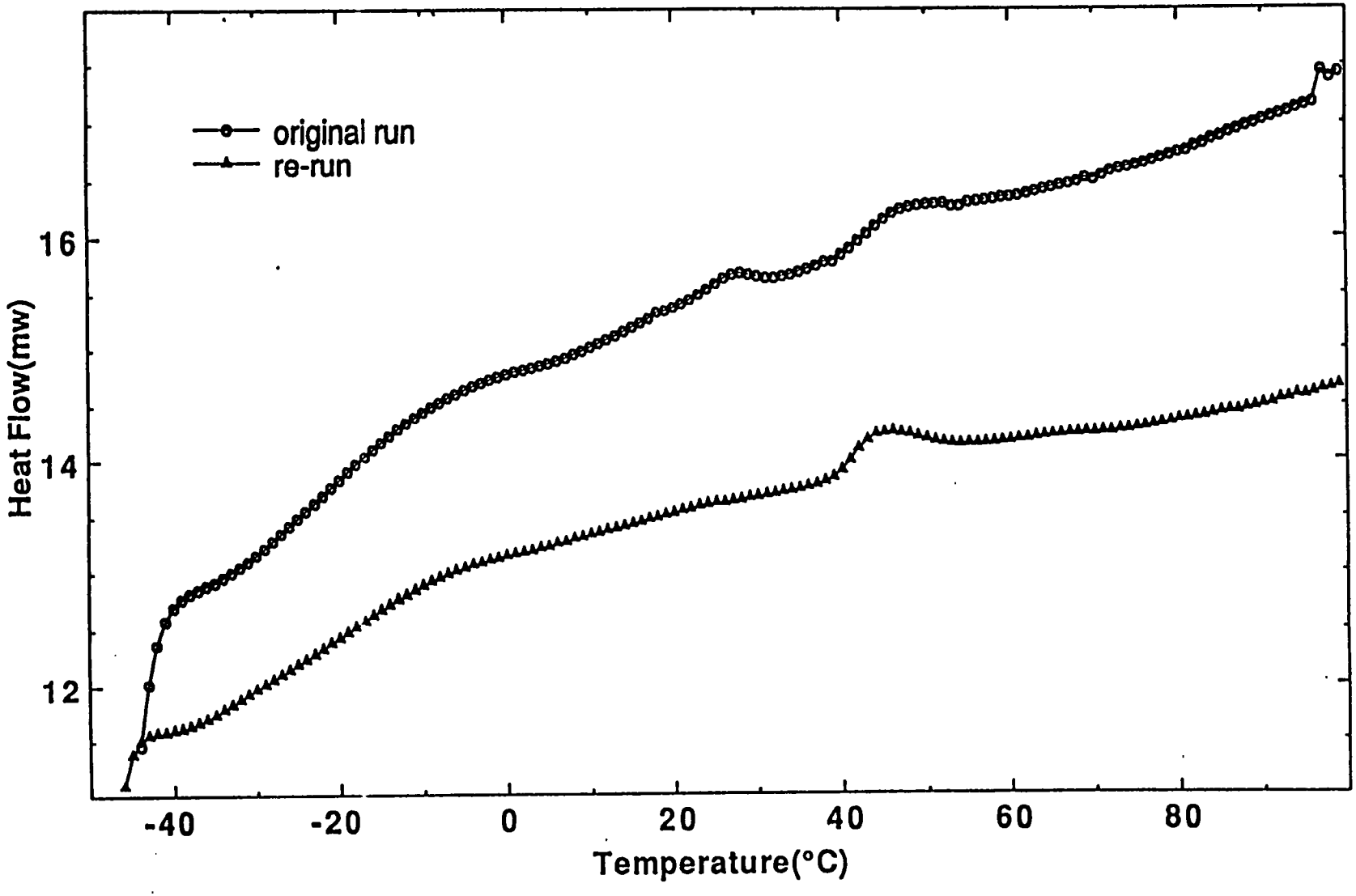

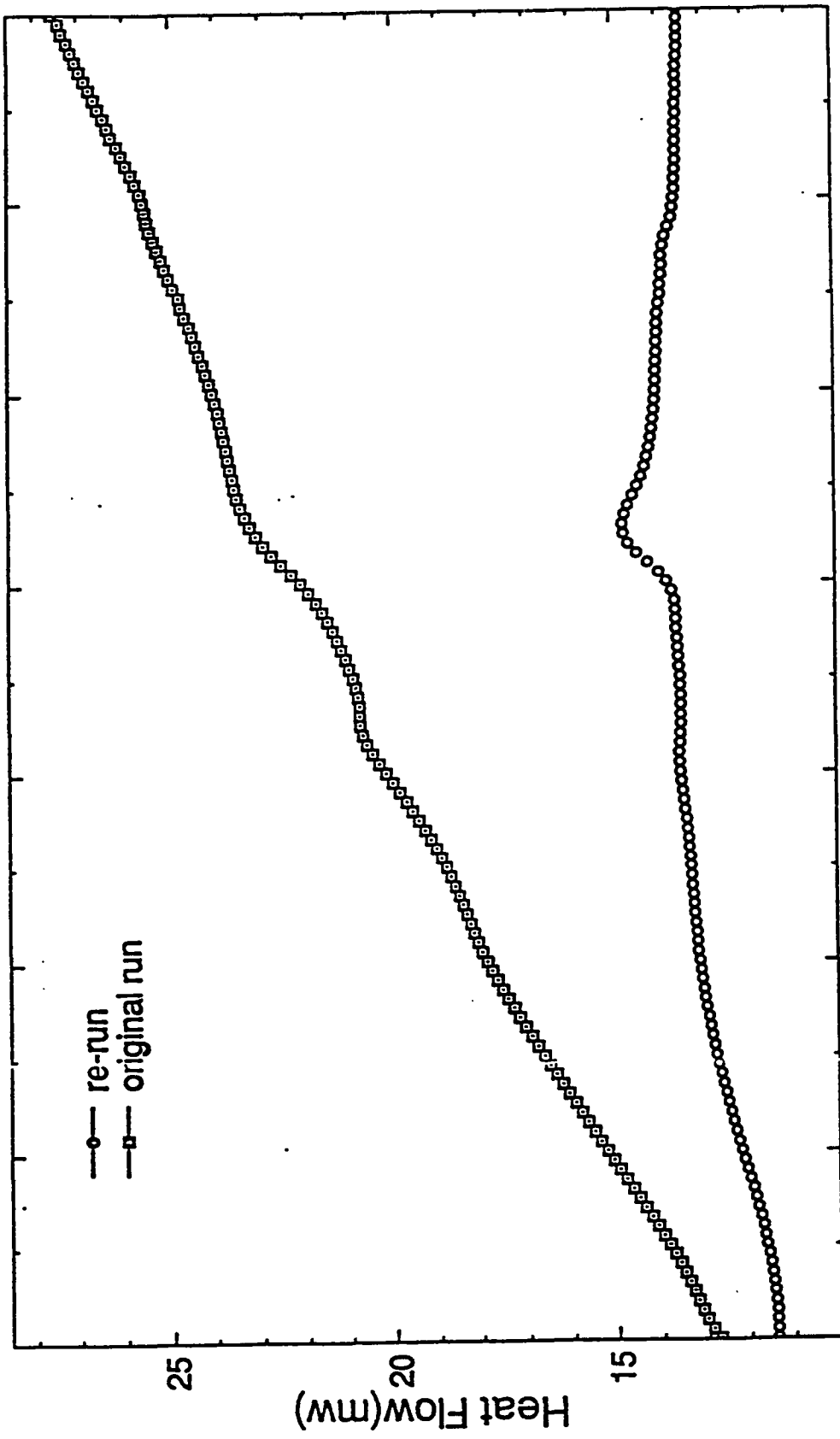

Figure 15. AAX original run and rerun

Figure 16 Slow Cooling Effect

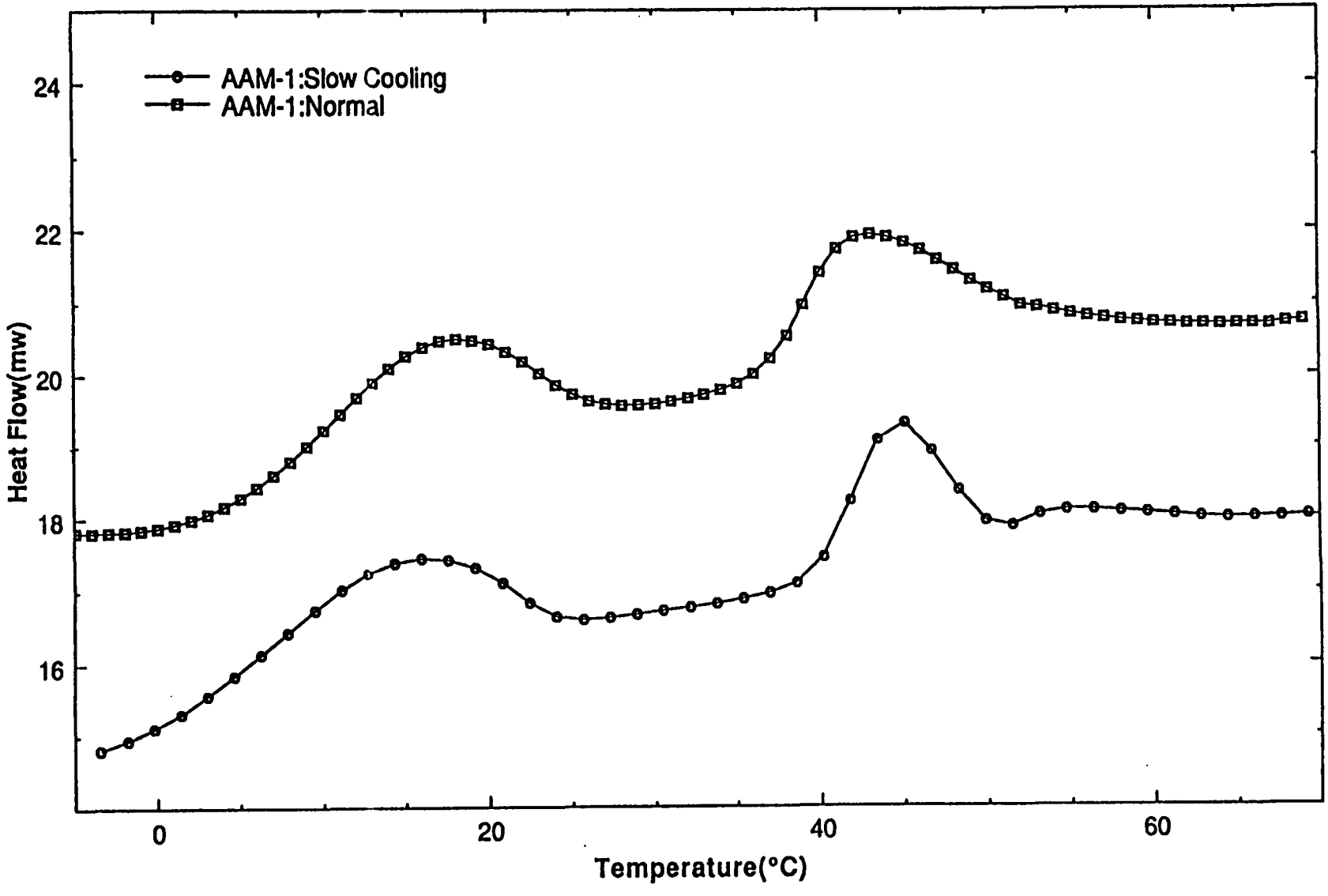

show a big increase. The combined area of both peaks seems to increase a little. Melting temperatures exhibit a small increase as heating rate increases.

Table 7. The Influence of Heating Rate on Melting*

Heating Rate	Tm1(°C)	Tm2(°C)	ΔH1/ΔH	ΔH(J/g)
5 (°C/min)	11.7	42.7	0.43	12.35
10(°C/min)	13.4	44.6	0.38	12.27
20(°C/min)	16.3	47.0	0.39	12.07

* The testing temperature range is from -50 to 100°C.

3.8 Other Miscellaneous Studies

It was reported that the asphalts have different mechanical properties after being stored at a low temperature (-15°C). We, therefore, tested a number of precooled asphalts to find out if there is any significant difference in their thermal behavior.

Figure 17 shows the DSC scans of cooled and uncooled AAM-1 samples. The scan of cooled samples as well as all other samples, did not show an increase in Tg, but rather, a slight decrease in Tg was observed. The first melting peak was unchanged and the second peak was shifted to a lower temperature.

DSC curves of samples treated by heating-cooling cycles are not easily reproduced. This is because we did not control the temperature at which samples were taken out of the heat-cool cycling device, therefore, samples may have very different final thermal histories.

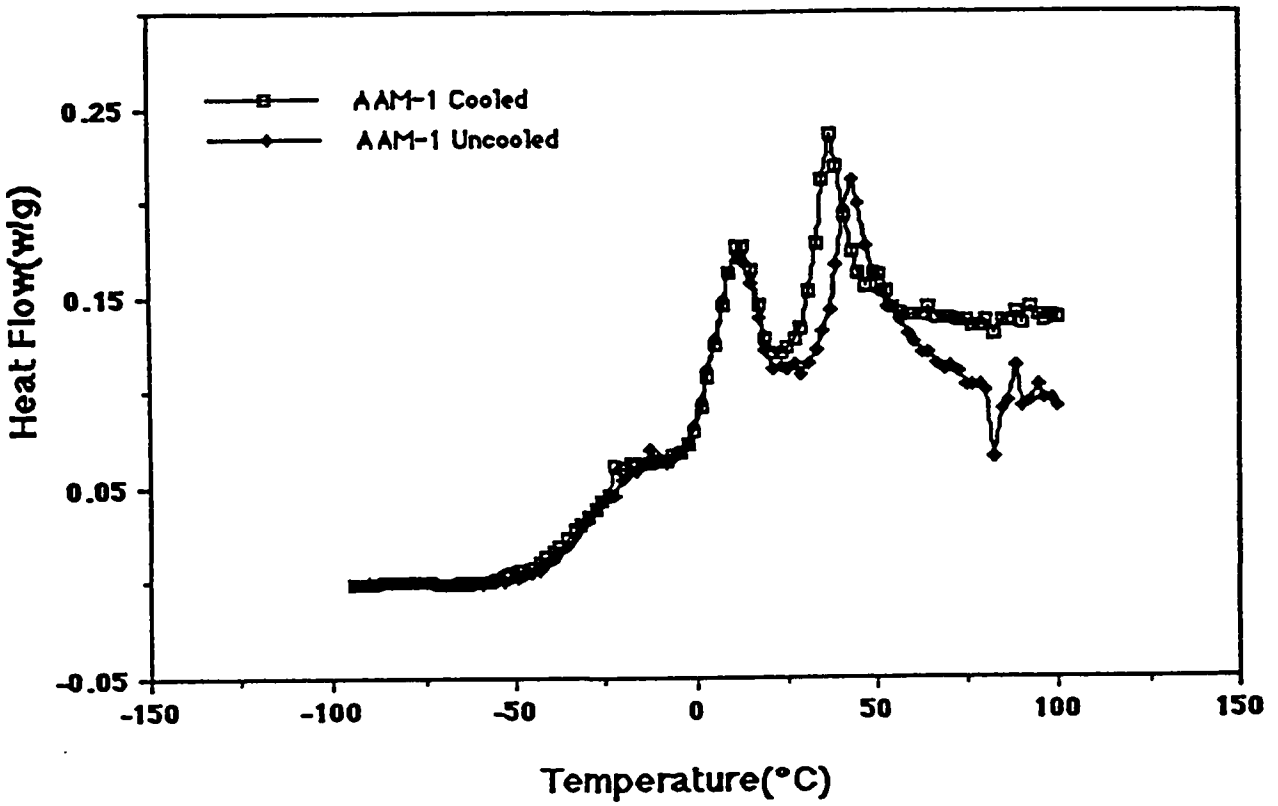

Figure 17. Cooling effect on AAM-1's thermal behavior.

4. Summary

Thermal properties of eight SHRP core asphalts and two types of fractions of several core asphalts have been measured using DSC. The Tg_{onset} for almost all the asphalts start from approximately -60°C. The main Tg, measured as the intercept temperature of the pretransition baseline and the slope line, lie in the range - 43±3°C for all asphalts except AAG-1 which has a significantly higher glass transition temperature.

In addition to the Tg transition, other thermal events have been observed. Immediately following the Tg transition a small exothermic effect has been seen for most of the asphalts. This is believed to be the result of crystallization which occurs during the heating process. Following this exothermic effect are two or three endothermic peaks. The third one usually appears as a shoulder on the second peak. Among all the asphalts tested, AAM-1, AAB-1 and AAF-1 showed much higher endothermic enthalpy than the others.

DSC testing of fractions based on their different chemical nature indicates that naphthene aromatics make a great contribution to the endothermic effect of the parent asphalt. Polar aromatics are presumed to be mainly responsible for the shoulder peak since they show a small endothermic effect at about the same temperature range. Asphaltene, due to its chemical nature, shows no endothermic effect. The thermal behavior of saturates is not clearly understood. More tests are needed in order to have a better understanding of this fraction's thermal behavior. Analysis of the SEC fraction's DSC results showed that the higher the molecular weight of the No. 1 fraction, the smaller the endothermic peak will be. This fraction is believed to be influenced by the high percentage of polycyclic aromatics in the asphalts. Analysis based on DSC results, composition data and molecular weight data for SEC and IEC neutral fractions also suggests that the average linear side chain length might be one of the key parameters affecting endothermic behavior.

Different thermal histories were found to have significant influence on asphalts' thermal behavior. Samples slowly cooled exhibit better separation between the two major melting peaks even though cooling did not go through the first melting peak. It has been speculated that this is a result of better separation of crystallizable materials.

Appendix

DSC Analysis Computer Program

1. Problems with the old DSC computer program

Since asphalts are very complicated system consisting a broad range of hydrocarbons with different molecular weights and chemical structures their DSC scans are much more difficult to analyze. Usually, the Tg value is determined by drawing two lines, each parallel to the linear portion of the DSC curve on either side of the transition and finding the intersection of the DSC curve at the midpoint between the two lines (see Figure 18). For those materials showing a well defined glass transition, Tg defined in this way would be relatively independent of the positions of T_1 and T_2.

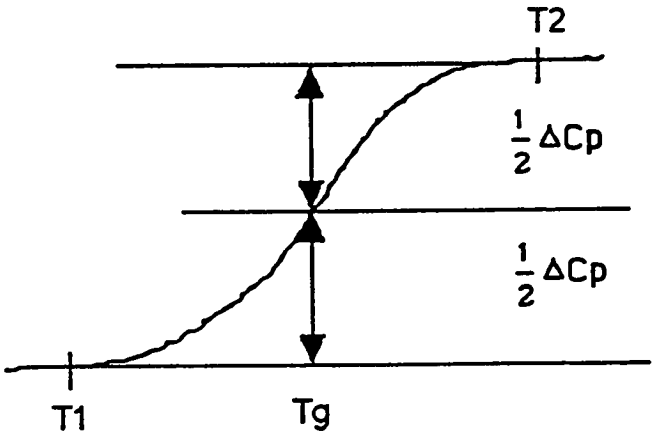

Figure 18. Half-height Tg definition.

Most asphalts, however, show poorly defined glass transitions. There are often an exothermic peaks closely followed the glass transition making it more difficult to draw baselines. For this type of DSC scan it is difficult to determine where T_2 should be located and the Tg value will be significantly different depending on T_2 location. Also, due to data fluctuations, slight differences in T_2 and/or T_1's position can result in a big difference in Tg. This is schematically demonstrated in Figure 19. One example showing Tg's dependence on T_2 is clearly shown in Table 8.

2. Major improvements of the new computer program:

A number of improvements including Tg calculation, curve manipulation, glass transition baseline removal and different peak area calculation methods have been made in the new computer program.

Improvement of Tg calculation is achieved by performing linear regression over as many operator selected data points as possible to obtain baselines required for Tg calculation. This method greatly reduces the dependence of Tg on individual data point. Also, adopting the baseline-slope intersection point as Tg gets rid of the problem with the exothermic effect for some asphalts. The reproducibility of Tg calculation is significantly improved with the new program and, as an example, the results of 10 independent Tg calculations on the same data set is listed in Table 9; the average Tg is -34.3°C with fluctuation range less than ± 0.7°C.

Table 9. Improved reproducibility of Tg calculation

No. of Calculation	Tg °C
1	-33.6
2	-34.5
3	-34.1
4	-35.0
5	-33.8
6	-34.3
7	-34.3
8	-34.7
9	-34.6
10	-34.2

The old computer program did provide functions to align the curve with different slopes of an arbitrarily selected line. The new program improved this alignment by allowing the operator to select data points to calculate the pre-glass transition baseline and subtract the baseline from the DSC curve (see Figure 20). Another important function introduced in the new program is to calculate the area separately for two overlapped peaks as shown in Figure 1. This function is now available in some of the newer DSC analysis programs.

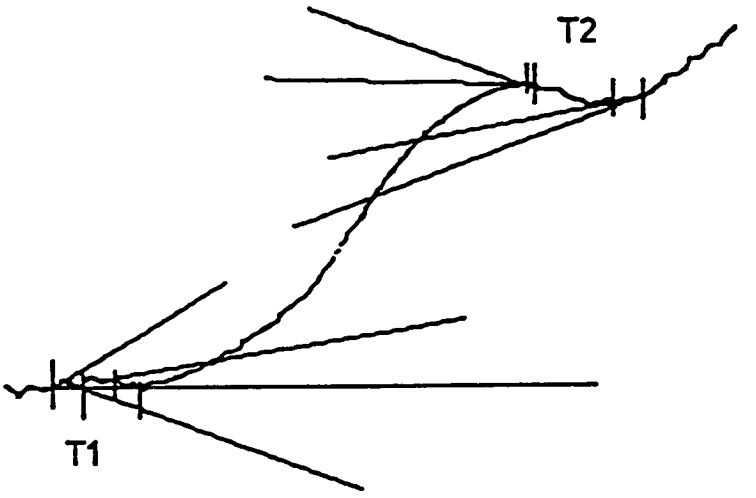

Figure 19. The influence of T_1 and T_2 positions and the data fluctuation on Tg value.

Table 8. The influence of T_2 on Tg values (with T_1 fixed)

T_2(°C)	$\|\Delta T_2\|$ (°C)	Tg(°C)	$\|\Delta Tg\|$ (°C)
-8.667		-42.4	
-8.534	0.123	-44.7	2.3
-6.000	2.534	-32.2	12.5
-3.334	2.666	-29.9	2.2
-2.934	0.400	-26.6	3.4
-2.800	0.134	-34.2	7.6
-2.667	0.133	-50.9	16.7
-2.534	0.133	-1.9	48.9
-2.400	0.134	-34.9	32.9

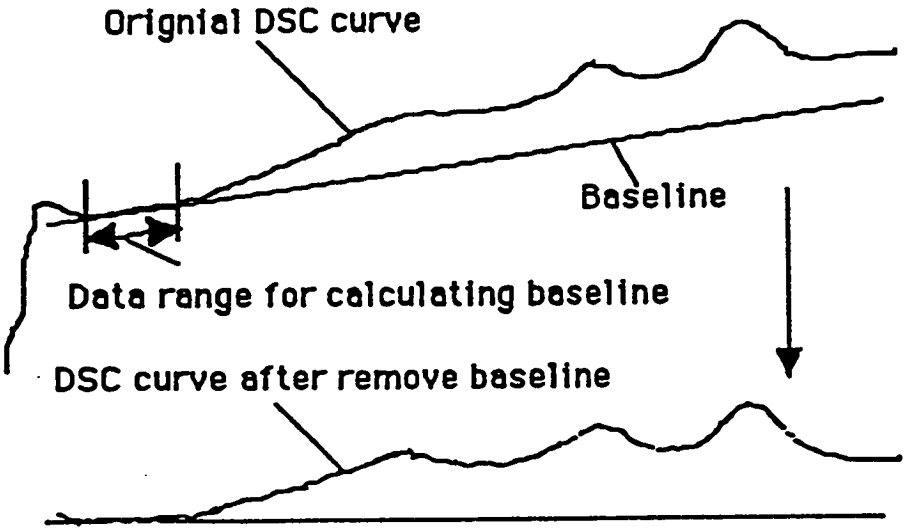

Figure 20. Curve alignment based on glass transition baseline

References

[1] R. J. Schmidt and E. M. Barrall, J. Inst. Pet., 51, 162 (1965)

[2] H. J. Connor and J. G. Spiro, J. Inst. Pet., 54, 137 (1968)

[3] F. Noel and L. W. Corbett, J. Inst. Pet., 56, 261 (1970)

[4] C. Giavarini and F. Pochetti, J. Thermal Analysis, 5, 83 (1973)

[5] H. K. Huynh, T. D. Khong, S. L. Malhotra and L. Blanchard, Anal. Chem. 50, 976 (1978)

[6] P. Claudy, J.M. Letoffe, B. Chague and J. Orrit, Fuel, 67, 58 (1988)

[7]. P. Claudy, J.M. Letoffe, G.N. King, J.P. Planche and B.Brule., Fuel Science and Technology Int'l., 9, 71 (1991)

[8] D. Kumari, Thermochimica Acta, 158, 71 (1990)

[9] L.W. Corbett, Anal. Chem., 41, 576, (1969)

[10] J.F. Branthaver, J.J. Duvall and J.C. Petersen, "Separation of SHRP Asphalts by Preparative Size Exclusion Chromatography", Symposium on Chemistry and Characterization of Asphalts, ACS 200th National Meeting, Washington, D.C., August 26-31, 1990.

[11] F.A. Barbour and J.F.Branthaver, "Supercritical Fluid Chromatography Separation of SHRP Asphalt Non-Polar Fractions", Symposium on Chemistry and Characterization of Asphalts, ACS 200th National Meeting, Washington, D.C., August 26-31, 1990.